People's Democratic Republic of Algeria
Ministry of Higher Education and Scientific Research

University M'Hamed BOUGARA – Boumerdes

Institute of Electrical and Electronic Engineering

Department of Electronics

Final Year Project Report Presented in Partial Fulfilment of the Requirements for the Degree of

MASTER

In **Telecommunication**

Option: **Telecommunications**

Title:

Design and Experimental Validation of a Microstrip Patch Antenna Array for Long-range Wireless Power Transfer Applications

Presented by:

- **Mr. Abdelali AROUS**
- **Mr. Hamza HAIF**

Supervisor:

Pr. Mouloud CHALLAL

Registration Number:……/2021

Dedication

Alhamdulillah, all praises to Allah for the strengths and His blessings in completing this dissertation

I'd like to dedicate this work to my beloved parents Dad ***Haif Hacen*** *and Mom* ***Affoune Hidi*** *whom have always been a constant source of love and support during the challenges of life, it is truly thanks to them I'm who I'm today*

To my sisters ***Asma*** *and* ***Khaoula*** *for filling my life with their pure love, support and innocent smiles. To my big brother* ***Mohammed*** *who believed in me*

To my friends ***B.Ziad, A.Ali, S.Abdel Djallil,*** *and* ***G.Firas*** *who has been with me through weal an woe*

Hamza

Dedication

This dedication is for my family, which was, is, and will be the greatest treasure I will have ever. To my parents, Father Arous Si Tahar and Mother Fatna Benziane, for making me the person I am and supporting me all the possible ways. Words cannot describe my love and appreciation for you.

To my siblings, the beloved one Nora and her incoming son Louay, I wish you a long and happy life. Wissam and Anes, the joy of our family. I love you infinitively.

To my childhood and company friends G. Mohammed, D. Amine, H. Haif, H. Tarek M. Abdellatif and G. Firas, we have spent great moments and share many memories with each other, I hope our friendship lasts forever.

To all my family members, particularly, Khaled and Ghani, I wish you success and happiness in your lives.

Abdelali

Acknowledgement

First and foremost, we are thankful to Allah, the most gracious, the most merciful for helping us to complete this modest work. It is our belief in him that guided us through the hardest times when it seemed impossible to go on.

Secondly, we would like to express our deepest gratitude to our supervisor **Pr. M. CHALLAL** for his help, guidance and support during the realization of this project. It has been an honor working with him.

We would like to express our sincere thanks and gratitude to **Dr. T. Maamria** and, **Ms. F. MOUHOUCHE** for their help and technical assistance during the designing and fabrication of the project.

Finally, we would like to thank all IGEE teachers and workers.

Abstract

In this work, a new microstrip antenna array for wireless power transfer (WPT) applications is designed, fabricated and measured. The proposed 1×4 antenna array operating at 2.45 GHz, based on defected ground structure (DGS), electromagnetic band gap (EBG), and multilayer parasitic elements, is designed using a commercial substrate FR-4 with relative dielectric constant of 4.3, thickness of 1.5 mm, copper thickness of 0.035 mm and loss tangent of 0.017.

The antenna offers -10 dB bandwidth of 180 MHz with beam width, gain, and directivity to be 24.7°, 10.90 dB and 13.30 dBi, respectively. Moreover, an SLL less than -20 dB, a return loss less than -35 dB, and polarization purity in the E-plane of –20.6 dB and in the H-plane of -80 dB are obtained with radiation efficiency of 53%.

KEYWORDS: microstrip antenna array**,** DGS, EBG, multilayer parasitic elements, WPT, FR-4 Substrate.

TABLE OF CONTENTS

Dedication ..... **I**

Acknowledgment ..... **III**

Abstract ..... **IV**

Table of Contents ..... **V**

List of Tables ..... **IX**

List of Figures ..... **X**

List of Abbreviations ..... **XIII**

List of Symbols ..... **XV**

General Introduction **1**

Chapter One: State of The Art

1.1 Introduction **4**

1.2 Radio Frequency and Microwaves **5**

1.3 Transmission Lines **6**

1.4 Microstrip Lines **6**

1.4.1 Overview **6**

1.4.2 Analysis Formulas **7**

a) The Effective Dielectric Constant **7**

b) Characteristic wavelength **8**

c) Guided Wavelength **8**

d) Propagation Constant **8**

e) Electric Length **8**

f) Phase Velocity **8**

1.5 Scattering Parameters **8**

1.6 Objectives and Organization **9**

1.7 Conclusion **10**

Chapter Two: Generalities About Microstrip Antenna

2.1 Introduction **12**

2.2 Microstrip Antennas **12**

2.2.1 Feed Techniques **13**

a) Microstrip Line Feed **13**

b) Coaxial Feed **13**

c) Aperture Coupled feed **13**

d) Proximity Coupled Feed **13**

2.2.2 Method of Analysis **14**

2.2.3 Advantages and Disadvantages **15**

2.3 Antenna Parameters and Characteristics **15**

2.3.1 Return loss **15**

2.3.2 Voltage Standing Wave Ratio **16**

2.3.3 Bandwidth **16**

2.3.4 Gain **16**

2.3.5 Directivity **17**

2.3.6 Input Impedance **17**

2.3.7 Radiation pattern **17**

2.3.7 Polarization **18**

2.4 Antenna Arrays **18**

2.4.1 Types of Antenna Arrays **18**

a) Linear **18**

b) Circular **19**

c) Planar **20**

d) Conformal **21**

2.4.2 Antenna Arrays Feeding **21**

2.5 Defected Ground Structure **22**

2.6 Parasitic Elements **22**

2.6.1 Electromagnetic Band Gap **23**

2.6.2 Multilayer parasitic Element **23**

2.7 Conclusion **24**

Chapter Three: Design of Microstrip Antenna Array

3.1 Introduction **26**

3.2 Design Procedure **27**

3.2.1 Design of the Antenna Array **27**

a) Single Element Antenna **27**

b) Two Elements MPA Array **29**

c) Four Elements MPA Array **31**

3.2.2 Performance Improvement of the Antenna Array ….…….... **33**

a) Using DGS ……..…… **33**

b) Using EBG ……..…… **35**

c) Using EBG + DGS ……..…… **37**

d) Using Multilayer Parasitic Elements……..…….. **38**

3.3 Fabrication and Experimental Results ……..…… **45**

3.4 Conclusion …….... **48**

General Conclusion …….. **49**

References ...……..... **XVII**

Appendix A ……..……..…….. **XXII**

Appendix B …….…….... **XXIV**

LIST OF TABLES

Table 1.1 Frequency Bands and Their Utilization **5**

Table 1.2 Comparison between Common Transmission Lines **6**

Table 2.1 Comparison between MPA's Analysis Methods **14**

Table 2.2 Advantages and Disadvantages of Microstrip Technology **15**

Table 3.1 RMPA Dimensions **28**

Table 3.2 RMPA's Simulation Results **28**

Table 3.3 Simulated Results of the Two-elements Antenna Array **30**

Table 3.4 Dimensions of the Four-elements Feeding Network **31**

Table 3.5 Simulated Results of Four-elements Antenna Array **31**

Table 3.6 Simulated Results of the Modified Four-elements Antenna Array **31**

Table 3.7 Comparison between Different Notch Widths **33**

Table 3.8 Comparison between the DGS's Elements' Widths **34**

Table 3.9 Comparison between EBG's Shapes Number **36**

Table 3.10 Comparison between Different EBG's Positions **37**

Table 3.11 Simulated Results of the EBG and DGS Combination **37**

Table 3.12 Four-elements Antenna Array Dimensions..... **38**

Table 3.13 Comparison between Different Heights of the One Parasitic Layer **39**

Table 3.14 Comparison between Different Heights of the Two Parasitic Layers **40**

Table 3.15 Comparison between Different Heights of the Three Parasitic Layers **40**

Table 3.16 Comparison between Different Designs **41**

Table 3.17 Performance Comparison of the Proposed Antenna Array with other Reported Works..... **47**

LIST OF FIGURES

Figure 1.1 Wireless Power Transfer Using EM Waves ……..…….... **5**

Figure 1.2 RF Spectrum ...…….…….... **5**

Figure 1.3 Transmission Lines: (a) Waveguide, (b) Microstrip Line, (c) Coaxial …..……..... **6**

Figure 1.4 Microstrip Line Structure ...……...……. **7**

Figure 1.5 Two-Ports Network's S-Parameters …..…….... **9**

Figure 2.1 Basic Structure of MPA ……..... **12**

Figure 2.2 Different Shapes of MPA's Radiating Patch……..…….…….... **13**

Figure 2.3 Different MPA's Feeding Techniques ……...……..... **14**

Figure 2.4 Radiation Pattern of MPA …… **17**

Figure 2.5 Linear Antenna Array …..……..... **19**

Figure.2.6 Circular Antenna Array …..…….…….... **20**

Figure.2.7 Planar Antenna Array …..…….…..... **20**

Figure 2.8 Conformal Antenna Array ……... **21**

Figure 2.9 Antenna Array's Feeding Techniques ..…….... **22**

Figure 2.10 Various DGS Models: (a) Spiral Head, (b) Arrowhead-Slot, (c) "H" Shape Slots, (d) A Square Open-Loop with a Slot in Middle Section, (e) Open-Loop Dumbbell (f) Interdigital DGS ……..... **22**

Figure 2.11 Rectangular MPA Surrounded by EBG Structures ....…….... **23**

Figure 2.12 Multilayer Parasitic MPA …… … **23**

Figure 3.1 RMPA with Inset Feed ……..... **27**

Figure 3.2 Microstrip Feed Line ……..... **28**

Figure 3.3 Radiation Pattern and the Geometry of Single Antenna ……..…. **29**

LIST OF FIGURES

Figure 3.4 Simulated Return Loss of the Single MPA **29**

Figure 3.5 Feed Network for a Two-elements Microstrip Antenna Array …..... **30**

Figure 3.6 Geometry of Two-elements Antenna Array along with its Radiation Pattern **30**

Figure 3.7 Simulated Return Loss of the Two-elements Antenna Array ……... **30**

Figure 3.8 Feeding Network for Four-elements Antenna Array ……..... **31**

Figure 3.9 Modified Four-elements Antenna Array after Introducing Bends ……..……. **32**

Figure 3.10 Radiation Pattern of the Modified Antenna Array …….……..... **32**

Figure 3.11 Simulated Return Loss of the Modified Antenna Array ...……..……... **32**

Figure 3.12 Proposed DGS's Shape: The Dumbbell ……..… **33**

Figure 3.13 Dumbbell DGS: (a) 3 Elements DGS, (b) 5 Elements DGS ……..…. **34**

Figure 3.14 Current Distribution of the Antenna Array: (a) With DGS, (b) Without DGS ... **35**

Figure 3.15 EBG Shapes: (a) First Shape, (b) Second shape, (c) Third shape …….. **35**

Figure 3.16 Final EBG Shape with its Dimensions ……..... **36**

Figure 3.17 Different EBG Positions Around the Antenna Array……..……..... **37**

Figure 3.18 Antenna Array Containing DGS and EBG: (a) Front View, (b) Back View **38**

Figure 3.19 The Proposed Multilayer Parasitic Elements ……..... **39**

Figure 3.20 Different Antenna Array Designs of Multilayer Parasitic Elements: (a) Three Layers, (b) One Layer, (c) Two Layers …….……..... **41**

Figure 3.21 Simulated Input Impedance of the Antenna Array …….…… **42**

Figure 3.22 Radiation Pattern of the Antenna Array in Polar and 3D forms…….…… **42**

Figure 3.23 Current Distribution of the Antenna Array ……..……... **42**

Figure 3.24 Simulated Gain Versus Frequency of the Antenna Array ……... **43**

LIST OF FIGURES

Figure 3.25 Simulated Axial Ratio of the Antenna Array ……..…….... **43**

Figure 3.26 E-Plane Radiation Pattern: (a) Co-Polarization, (b) Cross Polarization …… **44**

Figure 3.27 H-Plane Radiation Pattern: (a) Co-Polarization, (b) Cross Polarization ……..... **44**

Figure 3.28 Electric Field Intensity of the Antenna Array ……..……. **45**

Figure 3.29 Photography of the Antenna Array; (a) Top View, (b) Back View ……..…. **45**

Figure 3.30 Photography of the Parasitic Layer; (a) Top View, (b) Back View ……..…. **45**

Figure 3.31 Final Prototype of the Proposed Antenna Array ……..……. **46**

Figure 3.32 Simulated and Measured S_{11} of the Proposed Antenna Array ……... **46**

Figure A.1 CST MWS Different Applications ……...……... **XXII**

Figure A.2 CST MWS Optimizer …….……... **XXIII**

Figure A.3 Frequency Response of Breakdown Voltages and The Predicted Critical Frequency ……...…..……...…… **XXIV**

LIST OF ABBRIVIATIONS

WSN	Wireless Sensor Network.
IOT	Internet of Things.
WPT	Wireless Power Transfer.
DC	Direct Current.
GSM	Global System for Mobile communication.
WLAN	Wireless Local Area Network.
LTE	Long Term Evolution.
WiMAX	Worldwide interoperability for Microwave Access.
Radar	Radio Detection and Ranging.
RFID	Radio Frequency identification.
EM	Electromagnetic.
TEM	Transverse Electromagnetic.
RF	Radio Frequency.
SLL	Side Lobe Level.
VSWR	Voltage Standing Wave Ratio.
EBG	Electromagnetic Band Gap.
DGS	Defected Ground Structure.
FR-4	Flame Retardant and 4 means fiber glass epoxy.
MPA	Microstrip Patch Antenna.
G	Gain.
D	Directivity.
BW	Bandwidth.

LIST OF ABBRIVIATIONS

AF	Array Factor.
VNA	Vector Network Analyzer.
CST MWS	Computer Simulation Technology Microwave Studio.
RMPA	Rectangular Microstrip Patch Antenna.
Sonar	Sound navigation and Ranging.
AR	Axial Ratio
$\mathbf{E_{br}}$	Electric Breakdown Threshold

W	Stripline Width.
t	Stripline thickness.
h	Substrate thickness.
ε_{eff}	Effective dielectric constant.
ε_r	Relative permittivity.
Z_0	Characteristic impedance.
Z_S	Source impedance.
Z_L	Load impedance.
Ω	Ohms.
λ_g	Guided wavelength.
λ_0	Free space wavelength.
f	Operation frequency.
β	Propagation constant.
π	Pi number.
v_p	Phase velocity.
c	Light velocity.
s	Seconds.
m	meters.
mm	millimeters.
l	Microstrip physical length.
θ	Electrical length.
μ	Micro (10^{-6}).
η	Nano (10^{-9}).
p	Pico (10^{-12}).
S_{ij}	S-parameter.
Δ	Determinant.
Γ_{in}	Input reflection coefficient.

LIST OF SYMBOLS

$\boldsymbol{\Gamma_{out}}$	Output reflection coefficient.
$\boldsymbol{\Gamma_S}$	Source reflection coefficient.
$\boldsymbol{\Gamma_L}$	Load reflection coefficient.
$\boldsymbol{w}$	Frequency variable.
$\boldsymbol{Hz}$	Hertz.
$\boldsymbol{dB}$	Decibels.
$\boldsymbol{dBi}$	Decibels per isotropic.
$\boldsymbol{F_H}$	High frequency.
$\boldsymbol{F_L}$	Low frequency.
$\boldsymbol{P_r}$	Reflected power.
$\boldsymbol{P_{in}}$	Input power.
$\boldsymbol{\psi}$	Progressive phase.

GENERAL INTRODUCTION

In wireless communications, antennas are considered the fundamental building in those systems. Antennas are used to transmit and receive electromagnetic waves propagating through air. Without antennas mobile communications and other applications that are surging nowadays such as Wi-Fi, Radar systems, and LTE would not see the light. For that reason, engineers and researchers have developed and designed many antennas for various usages. The most common antenna type is the microstrip patch antennas which are light weight, low cost, and easy to fabricate. All those advantages made MPAs the most developed antennas nowadays.

Today's antennas are grouped together to form arrays to increase the gain and directivity, which are critical parameters in many applications like wireless power transfer (WPT) and satellite communications. Antenna arrays have many types and design's techniques, which provide the designers flexibility and space for modifications. WPT deploys antenna arrays which provide high output in terms of gain, directivity, and operating range. For that, many researchers suggested a variety of designs to meet the requirements and demands of WPT applications [1-2]. Increasing the number of the array elements will generate high gain, but at the expanse of size and cost. Although MPAs have many advantages over other types of antennas, but they provide low gain and efficiency which obstruct the required high-performance of the antenna arrays. To overcome the low gain and efficiency of MPAs, many techniques like electromagnetic band gap (EBG) [3], multilayer parasitic elements [4], and defected ground plane (DGS) [5] are used in the design of antenna arrays.

Among the various types of antenna arrays, linear arrays are the most used since they are easy to design and fabricate although they deliver low gain and side lobes level. The frequency range from 2 to 4 GHz with wavelength between 7.5 to 15 cm, belongs to the S frequency band which is widely used in many applications including Wi-Fi and WPT since it consumes low power, supports high data transmission rate and long ranges, and uses simple hardware unlike high frequencies which require more sophisticated devices.

The aim of this work is to design, simulate, and fabricate an MPA array operating at 2.45 GHz frequency for WPT applications. Techniques like DGS, EBG, and multilayer parasitic elements are used to enhance the array's performance. The used substrate material is FR-4 with relative permittivity constant of 4.3, a height of 1.5 mm, and loss tangent of 0.017. The simulation is carried on CST MWS software (Appendix A).

GENERAL INTRODUCTION

This report is organized as follows:

Chapter 1, introduces a wireless power transfer theory and applications, and a brief literature review of Radio Frequency Theory.

Chapter 2, provides some of the basic concepts and theories of microstrip patch antennas and antenna arrays. Including feeding techniques, some applications, methods of analysis, and antenna arrays types. Important antenna parameters are also introduced.

Chapter 3, details the design, simulation, and fabrication of the microstrip patch antenna array, with a break through all steps from the single element MPA to the four elements MPA array. A comparison with other works will be provided also along future work.

CHAPTER ONE

State of The Art

1.1 Introduction

Radio frequency is a major field of research and development since it supports applications in the evolving field of communications such as cellular networks, GSM, WLAN, LTE, Wi-Fi, WiMAX, medical equipment, satellite communication, radar systems, and space navigation. These applications run on devices that operate at frequencies ranging from 30 KHz to 300 GHz, which is the range of radio frequency bands.

After the speeding development of wireless technologies like mobile communications, and wireless sensor networks (WSNs) such as the internet of things (IoT), which is used in automated industries, smart cities, highways, and self-driving cars, the need for wireless power supply became a necessity. Wireless power transfer (WPT) has been introduced a century ago by Nikola Tesla [6] as a potential transmission of electrical energy over a wireless medium. The transmitter is usually connected to a power source, then it generates a time-varying electromagnetic field EM (generally using antennas) that propagates through space to a receiver which converts the EM's power to DC then supply it to a connected load. WPT is used around us nowadays in many applications such as telemetry, satellite communication, wearable electronics, charging rechargeable batteries, and RFID tags [7].

The power transferred was usually in the range of microwatts to milliwatts, after that it was deployed for higher-power applications from few watts to several kilowatts. WPT is preferred over the conventional usage of copper wires and batteries for the following reasons:

- The increasing mobility of devices and power supply.
- Safety of electronic devices.
- Useful when interconnecting wires are hazardous or not possible.

WPT techniques are divided into two categories, near-field and far-field. The near-field power is transferred by magnetic fields using inductive coupling, most of the time over short distances this technique is used in charging phones and RFID tags [8]. In our case it is the far-field technique shown in figure 1.1 [9] which interests us. Power is transferred by EM waves for long distances, this technique requires the utilization of high directive antennas such that the power is concentrated in the main lobe. Far-field WPT antennas operate in GHz frequencies and must provide high gain and directivity so they deliver power as much as possible. The far-field WPT system is composed of a transmitting unit connected to a power supply and an antenna array that radiates the EM waves to the direction of the receiving unit, the receiving unit consists

of a rectenna that receives the EM waves then converting them to DC using a rectifying and filtering units [10].

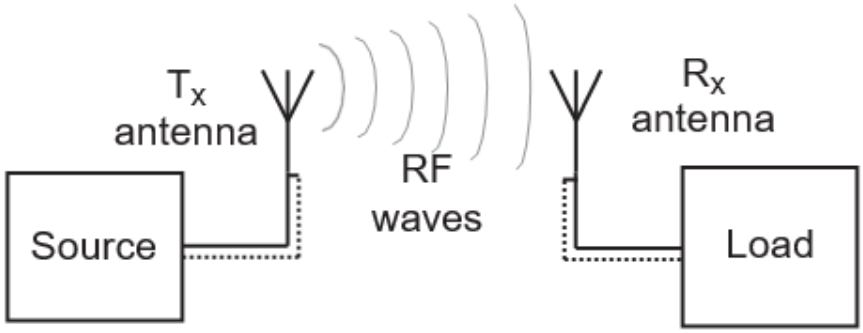

Figure 1.1 Wireless Power Transfer Using EM Waves.

1.2 Radio Frequency and Microwaves

RF appliances use signals that are in the form of EM waves for transmission and reception. Those signals' frequencies lie in the range of EM spectrum between 30 KHz and 300 GHz, as shown in figure 1.2.

Figure 1.2 RF Spectrum.

The term microwaves refer to EM waves with a wavelength in the range from 100 cm to 1 mm. Millimeter waves (1 – 10mm) are also called microwaves since their technologies are similar. Microwaves and millimeter waves are divided into several frequency bands depending on the corresponding wavelength. Table 1.1 [11] shows frequency bands.

Designation	Frequency range	Wavelength range	Typical uses
L band	1 to 2 GHz	15 cm to 30 cm	Military telemetry, GPS, mobile phones (GSM), amateur radio
S band	2 to 4 GHz	7.5 cm to 15 cm	Weather radar, surface ship radar, and some communications satellites
C band	4 to 8 GHz	3.75 cm to 7.5 cm	Long-distance radio telecommunication
X band	8 to 12 GHz	25 mm to 37.5 mm	Satellite communications, radar, terrestrial broadband, space communications, amateur radio

Table 1.1 Frequency Bands and Their Utilization.

1.3 Transmission Lines

The media carrying electrical energy are called transmission lines [12]. These connecting links have significant importance in the analysis and design of microwave circuits. They come in different types as shown in figure 1.3 [13].

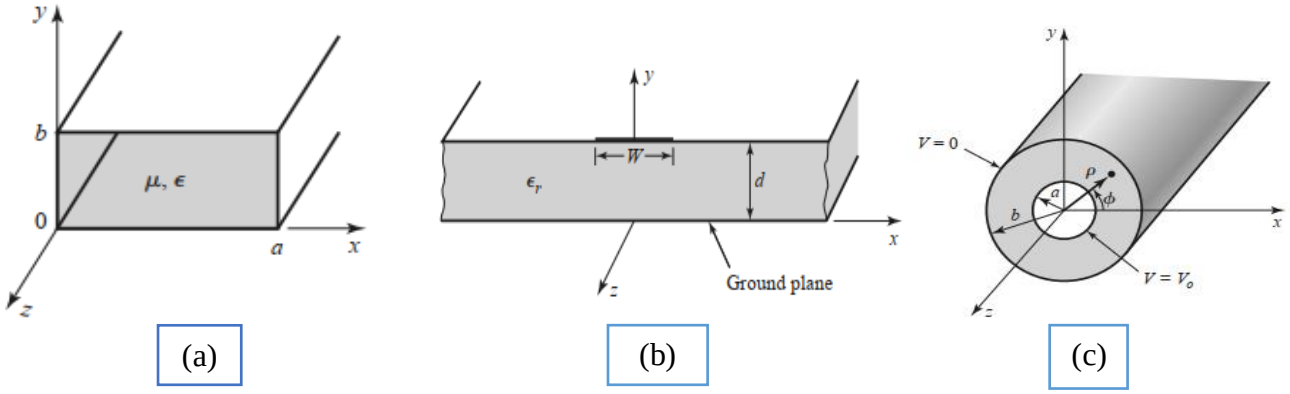

Figure 1.3 Transmission Lines: (a) Waveguide, (b) Microstrip Line, (c) Coaxial.

The decision for transmission line type selection is based on many factors such as performance and ease of fabrication and implementation. Generally, microstrip lines are the most widely used. Table 1.2 [14] shows a comparison between common transmission lines.

Characteristic	Coax	Waveguide	Stripline	Microstrip
Preferred mode	TEM	TE10	TEM	Quasi-TEM
Other modes	TE, TM	TE, TM	TE, TM	TE, TM
Dispersion	None	Medium	None	Low
Bandwidth	High	Low	High	High
Loss	Medium	Low	High	High
Power Capacity	Medium	High	Low	Low
Physical size	Large	Real large	Medium	Small
Fabrication ease	Medium	Medium	Easy	Real easy
Component integration	Hard	Hard	Fair	Easy

Table 1.2 Comparison between Common Transmission Lines.

1.4 Microstrip Line

1.4.1 Overview

Microstrip was developed by ITT federal telecommunication laboratories in Nutley New Jersey, it was published by Grieg and Engelmann in December 1952 as a competitor to stripe line [15].

As has been mentioned by [13], the first microstrips did not support non-TEM wave propagation because of thick substrates. Therefore, the results were unpredictable. Later thinner versions of microstrip became popular in the 1960s. Microstrip lines became important for both RF and microwave circuit design, primarily because they can be fabricated by photolithographic processes and are easily integrated with other microwave devices [16]. With substrate's height of a few percent of a wavelength, radiations can be minimized without forcing strip width to be narrow. The dominant mode is forced to be Quasi-TEM (hybrid) instead of TEM, leading to a phase velocity, characteristic impedance, and frequency dependency of the field variation in the guide cross-section [17].

Microstrip line structure illustrated in figure 1.4 [18], consists of a conductive strip of width (W), length (L), and thickness (t) that lies on the top of a wide ground plane usually made of copper and separated by a dielectric layer called substrate of height (h) and dielectric constant (ε_r) [17]. Microstrip line does not support TEM waves propagation because of relative permittivity ε_r which is always greater than unity. For that, waves in the air propagate faster than those within the dielectric.

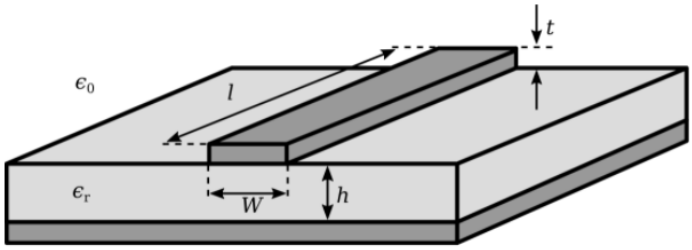

Figure 1.4 Microstrip Line Structure.

1.4.2 Analysis Formulas

a) The Effective Dielectric Constant: The effective dielectric constant ε_{eff} is less than the substrate dielectric constant ε_r, because of the existence of some part of fields from the microstrip conductor in the air. It is calculated as follows [13]:

When $(\frac{W}{h}) < 1$

$$\varepsilon_{eff} = \frac{\varepsilon_r+1}{2} + \frac{\varepsilon_r-1}{2}\left[\left(1+\frac{12h}{W}\right)^{-1/2} + 0.04\left(1-\frac{W}{h}\right)^2\right] \quad (1.1)$$

When $(\frac{W}{h}) \geq 1$

$$\varepsilon_{eff} = \frac{\varepsilon_r+1}{2} + \frac{\varepsilon_r-1}{2}\left(1+\frac{12h}{w}\right)^{-1/2} \quad (1.2)$$

Where w is the width of the strip and h is the substrate's height.

b) Characteristic Impedance: characteristic impedance of the microstrip is calculated as follows [15]:

When $(\frac{W}{h}) < 1$

$$Z_0(\Omega) = \frac{60}{\sqrt{\varepsilon_{eff}}} ln\left(\frac{8h}{W} + \frac{W}{4h}\right) \quad (1.3)$$

When $(\frac{W}{h}) \geq 1$

$$Z_0(\Omega) = \frac{120\pi}{\sqrt{\varepsilon_{eff}}\left(\frac{w}{h}\right)+1.393+0.667ln\left(1.444+\left(\frac{w}{h}\right)\right)} \quad (1.4)$$

c) Guided Wavelength: wavelength is inversely proportional to the frequency. Knowing that λ_0 is the wavelength in free space, the guided wavelength is given by [20]:

$$\lambda_g(m) = \frac{\lambda_0}{\sqrt{\varepsilon_{eff}}} \quad (1.5)$$

If the frequency is in Gigahertz (GHz), the guided wavelength can be obtained in millimeters directly by [21]:

$$\lambda_g(mm) = \frac{300}{f\sqrt{\varepsilon_{eff}}} \quad (1.6)$$

d) Propagation Constant: propagation constant β is given by [13]:

$$\beta = \frac{2\pi}{\lambda_g} \quad (1.7)$$

e) Electrical Length: for a physical length l, electrical length is defined as [22]:

$$\theta = \beta l \quad (1.8)$$

Hence, $\theta = \pi/2$ when $l = \lambda_g/4$, and $\theta = \pi$ when $l = \lambda_g/2$. These so-called quarter-wavelength and half-wavelength microstrip lines are critical for microstrip feeding network design [23].

f) Phase Velocity: phase velocity is given by [13]:

$$v_p(m/s) = \frac{W}{\beta} = \frac{c}{\sqrt{\varepsilon_{eff}}} \quad (1.9)$$

Where c is the light velocity in free space (3×10^8 m/s).

1.5 Scattering Parameters

Scattering parameters (also called S-parameters) describe the behavior of linear microwave networks. They quantify how much RF energy propagates through a multi-port network [24], usually two-port networks. If an RF signal is incident on one port, part of the signal gets reflected and the other part comes out from another port.

We express S-parameters mathematically as complex coefficients with magnitude and phase in a matrix format. We are interested in the magnitude only most of the time. The number of rows and columns is equal to the number of ports. S_{ij} is an element of the s-parameters matrix, where 'j' refers to the exciting port (input port) and 'i' refers to the output port.

For a two-port network shown in figure 1.5, S-parameters are given by [25] [26]:

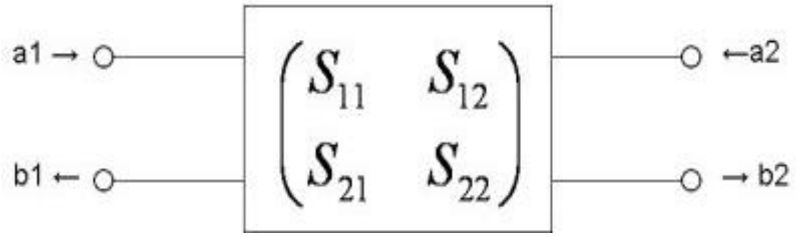

Figure 1.5 Two-Ports Network's S-Parameters

$$\begin{pmatrix} b_1 \\ b_2 \end{pmatrix} = \begin{pmatrix} S_{11}S_{12} \\ S_{21}S_{22} \end{pmatrix} \begin{pmatrix} a_1 \\ a_2 \end{pmatrix} \rightarrow \begin{matrix} b_1 = S_{11}a_1 + S_{12}a_2 \\ b_2 = S_{21}a_1 + S_{22}a_2 \end{matrix} \quad (1.10)$$

Where a_n and b_n are normalized usually as:

$$a_n = \frac{V_{n+}}{\sqrt{Z_{0_n}}}, b_n = \frac{V_{n-}}{\sqrt{Z_{0_n}}} \quad (1.11)$$

We can calculate the input and output reflection coefficients from the s-parameters as follows:

$$\Gamma_{in} = \frac{S_{11} - \Delta\Gamma_L}{1 - S_{22}\Gamma_L} \quad \text{and} \quad \Gamma_{out} = \frac{S_{22} - \Delta\Gamma_S}{1 - S_{11}\Gamma_S} \quad (1.12)$$

where:

$$\Gamma_S = \frac{Z_S - Z_0}{Z_s + Z_0} \quad (1.13)$$

$$\Gamma_L = \frac{Z_L - Z_0}{Z_L + Z_O} \quad (1.14)$$

$$\Delta = S_{11}S_{22} - S_{12}S_{21} \quad (1.15)$$

Practically the S-parameters are obtained for the two-port networks by using the vector network analyzer (VNA).

1.6 Objectives

Our objectives in this work is to design, simulate and fabricate a MPAs array for WPT applications at 2.45 GHz resonance frequency. The antenna array is supposed to provide high

gain and directivity along with low side lobe level (SLL) suppression, which are the most important parameters when working on WPT applications. High directive antenna arrays are critical for power transfer since they focus the EM energy into the main lobe leading to a reduction of the wasted energy on the side lobes. Our antenna array is designed using microstrip technology and is supposed to resonate at 2.45 GHz with a reflection coefficient less than -10 dB, SLL is required to be less than -20 dB to meet WPT requirements. The gain must be in the range between 9 dB and 11 dB and the directivity should be more than 12 dB, the efficiency also needs to be more than 50 %. Techniques like defected ground structure (DGS), electromagnetic band gap (EBG), and multilayer parasitic elements will be used to increase the gain. The antenna array is fabricated on a standard cost-effective FR-4 substrate of thickness 1.5 mm, a dielectric constant $\varepsilon_r = 4.3$, and tangent loss of 0.017 which is widely used in S-band applications.

1.7 Conclusion

In this chapter we have discussed some basic knowledge about wireless power transfer with its applications and categories. Radio frequency is the field covering devices and applications operating on frequencies from 30 KHz to 300 GHz. Frequencies can be classified based on the corresponding wavelength, where there exist microwaves and millimeter waves frequencies having a wavelength between 100 cm to 1 mm.

CHAPTER TWO

Generalities on Microstrip Antenna Arrays

2.1 Introduction

An antenna is an electronic device that directs incoming and outgoing EM waves. Antennas (also called aerials) have a critical role in radio, television, radar systems, and wireless communication devices. The first antenna was devised by Heinrich Hertz in the late 1880's [27], and since then a huge surge in the development and researches of antennas has occurred.

Antennas come in different shapes and sizes depending on the utilization. Generally, devices which operate at high frequencies deploy small antennas. The most common types of antennas are dipole, horn, loop, wire, and aperture antenna. Nowadays MPAs are the mostly used and deployed ones for their ease of fabrication and design. In this chapter we will go through a general review about MPA's theory and antenna parameters along with array types and feeding techniques.

2.2 Microstrip Antennas

MPAs are planar antennas which have two-dimensional flat structure. MPAs are the most favorited among antenna designers for their ease of fabrication and integration, flexibility and simplicity. For those reasons they have various applications in mobile and satellite communications, global positioning system (GPS), RFID, and rectenna applications [28]. MPAs are extensively developed and researched over the last four decades since they were introduced first in the early 1980's by Deschamps [29].

Microstrip patch antenna's structure shown in figure 2.1 [30], consists an area of a metallization above a ground plane of a high conductivity metal, usually copper and separated by a thin dielectric substrate of height 'h' and permittivity ε_r, fed using one of the techniques that will be discussed later.

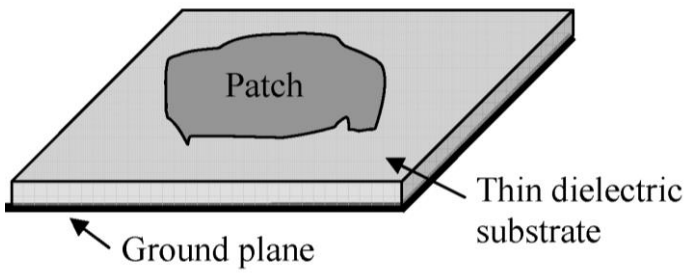

Figure 2.1 Basic Structure of MPA.

The geometry of the radiating patch leads to different shapes of the MPA as shown in figure 2.2 [31]:

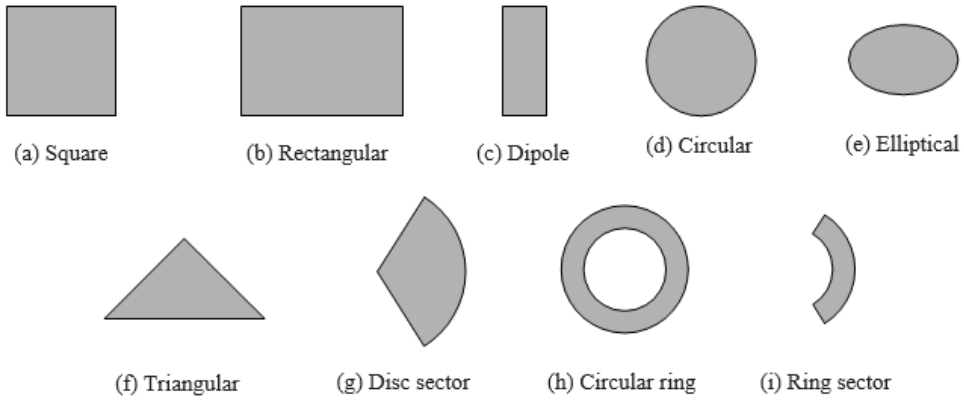

Figure 2.2 Different Shapes of MPA's Radiating Patch.

2.2.1 Feed Techniques

We can classify MPA feeding techniques into two major categories: contacting and non-contacting. Contacting feeding is where the power is being directly fed to the radiating patch, like microstrip line and coaxial line. In the other side, non-contacting feeding is where the power is fed by EM coupling between the radiating patch and the microstrip line, aperture coupling and proximity coupling are the most popular among this category [32].

a) Microstrip Line Feed: the conducting strip is directly connected to the radiating patch and can be designed using microstrip line design's techniques. An inset cut in the patch can be added to match the patch's impedance to the one of the microstrip; then the feeding will be called inset.

b) Coaxial Feed: the inner conductor of the coaxial connector feeds the radiating patch from underneath through the dielectric while the outer conductor is connected to the ground plane. The position of the feeding can be changed to control the input impedance. The drawback of this feeding is that it requires ironing the coaxial cable to the patch leading to mismatches.

c) Aperture Coupled Feed: the radiating patch is separated from the microstrip feed line by the ground plane with an aperture to transmit energy to the antenna. We use two substrates; the upper one we chose it with low ε_r for better radiation and the lower one with high ε_r to avoid spurious radiations. This technique is difficult to fabricate due to the usage of two substrates.

d) Proximity Coupled Feed: in this technique, there are also two substrates and the microstrip feed line is between them whereas the radiating patch is on the top of the upper substrate. Figure 2.3 [30] shows the all the above-mentioned feeding techniques.

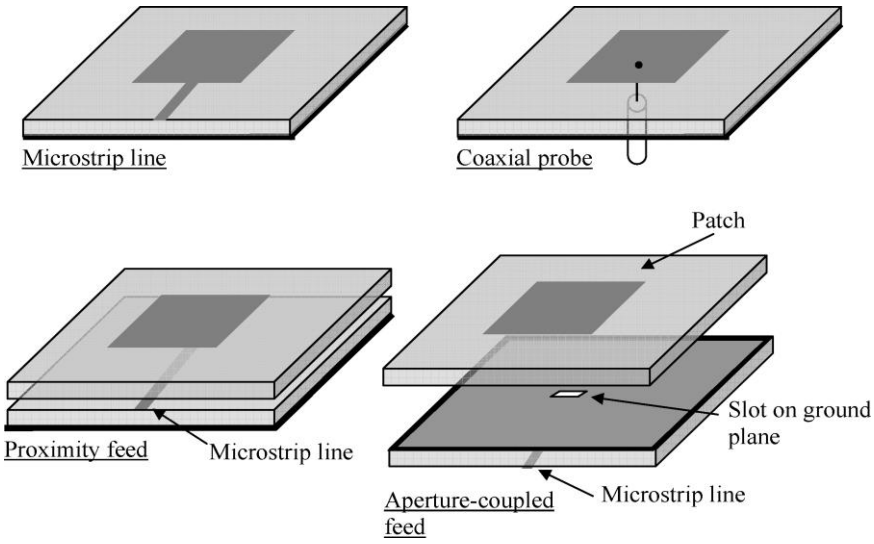

Figure 2.3 Different MPA's Feeding Techniques.

2.2.2 Methods of Analysis

There exist many methods for the analysis of the microstrip antenna such as moments method, finite elements method, and segmentation method. However, the most common methods are the transmission lines, cavity, and the full-wave [31].

The moment method is a numerical technique that is applied to regular shapes only (rectangular, circular and elliptical shapes). The finite element method in the other hand is also a numerical technique that can be used for arbitrary shapes [33], but both of these techniques are time consuming and computationally expensive. Segmentation method which was proposed by Okashi et al [34], uses expansion functions that are eigen functions of the corresponding segments of the partitioned shape. A comparison between the full-wave, cavity and transmission line methods are provided in table 2.1 [31]:

Technique	Transmission line	Cavity	Full-wave
Physical insight	good	good	bad
Accuracy	low	Medium	High
Coupling method	Hard	Hard	Easy
Difficulty	Easy	Complex	Complex

Table 2.1 Comparison between MPA's Analysis Methods.

2.2.4 Advantages and Disadvantages

MPAs as any technology, have a variety of advantages along with some disadvantages. By understanding them well we can adjust the design according to what we can achieve by the microstrip technology. Table 2.2 [28] shows the merits and demerits of MPA:

Merits	Demerits
Low-cost and small size.	Excitation of surface waves.
Ease of fabrication and design.	Low power handling capacity.
Supports linear and circular polarization.	Polarization purity is difficult to achieve
Can operate at high frequencies in dual and triple bands.	Provides low gain, efficiency, and narrow bandwidth.
Light weight and the ease of integration in microwave integrated circuits MICs.	Large ohmic loss in the feeding structure of the arrays.
Minimization of excitation of undesired modes.	Extraneous radiations from feed lines and junctions.

Table 2.2 Advantages and Disadvantages of Microstrip Patch Antennas.

2.3 Antenna Parameters and Characteristics

2.3.1 Return Loss

Return loss is a measurement of the power of the reflected wave from a transmission line. Usually measured on a logarithmic scale dB. Return loss S_{11} is an S-parameter and can be calculated using equation 2.1 [35]:

$$RL(dB) = 10log\left(\frac{P_r}{P_{in}}\right) = 20log\left|\frac{Z_{in}-Z_0}{Z_{in}+z_0}\right| \quad (2.1)$$

where:

P_r is the reflected power in Watts, P_{in} is the incident power in Watts. The negative sign indicates the loss, generally -10 dB is an acceptable return loss and the less it is the better.

2.3.2 Voltage Standing Wave Ratio

VSWR is a numerical value that describes how well the antenna impedance is matched to the transmission line's impedance it is connected to. VSWR is a function of the reflection coefficient, equation 2.2 [13] defines VSWR:

$$VSWR = \frac{1 + |\Gamma|}{1 - |\Gamma|} \tag{2.2}$$

VSWR can also be written in terms of V_{max} and V_{min} as follows:

$$VSWR = \frac{Vmax}{Vmin} = \frac{1 + \rho}{1 - \rho} \tag{2.3}$$

Where Γ is the reflection coefficient or S_{11} and ρ is the magnitude of Γ.

2.3.3 Bandwidth

The bandwidth BW is the range of possible frequencies over which the antenna can radiate or receive energy. It is measured in Hz and typically defined where the VSWR is less than 2:1. Equation 2.4 [36] defines the bandwidth:

$$BW = \frac{f_H - f_L}{f_c} \tag{2.4}$$

Where f_H is the highest frequency in the band, f_L is the lowest frequency in the band, and f_c is the center frequency in the band. In this way, bandwidth is constant relative to frequency. If the bandwidth was expressed in absolute units of frequency, it would be different depending upon the center frequency. Different types of antennas have different bandwidth limitations [36].

2.3.4 Gain

Antenna gain (G) describes how much power is radiated in the direction of the peak radiation. Gain is a dimensionless quantity, but it is measured in dB. It is preferred to have the highest possible gain for an acceptable antenna design. The gain can be obtained using equation 2.5:

$$G(\phi, \theta) = 4\pi \frac{U(\phi,\theta)}{P_{in}} \tag{2.5}$$

Where: $U(\phi, \theta)$ is the normalized radiation pattern and P_{in} is the input power in watts. Gain is given in reference to a standard antenna [36]. The two most common reference antennas are the isotropic antenna and the resonant half-wave dipole antenna.

2.3.5 Directivity

The directivity (D) is a parameter given in dBi measuring the ability of concentrating energy in a particular direction when transmitting, or to receive energy better from a particular direction when receiving. Equation 2.6 [31] provides a mathematical formula for the directivity:

$$D(\theta,\phi) = 4\pi \frac{F(\theta,\phi)}{\int_0^{2\pi} \int_0^{\pi} F(\theta,\phi) \sin\theta d\theta d\phi} \tag{2.6}$$

In some applications, the directivity is preferred to be high like in wireless power transmission. However, in other applications it is required to be low, like mobile devices communication. The directivity is related to the gain by equation 2.7 [31]:

$$G = \varepsilon_{antenna} D \tag{2.7}$$

$\varepsilon_{antenna}$ is the antenna radiation efficiency, which is always less than unity.

2.3.6 Input Impedance

Z_{in} is the impedance presented by an antenna at its terminals, or the ratio of the voltage to current at a pair of terminals, or the ratio of the appropriate components of the electric to magnetic fields at a certain point [31]. It's represented as follows:

$$Z_{in} = R_{in} + jX_{in} \tag{2.8}$$

Where R_{in} is the real part of the input impedance, and X_{in} is the imaginary part.

2.3.7 Radiation Pattern

Radiation pattern describes the strength of the radiated field distribution as a function of space coordinates. In most cases, it is represented in 3D or 2D in the far-field region and usually in polar format. Figure 2.4 shows the radiation pattern of MPA.

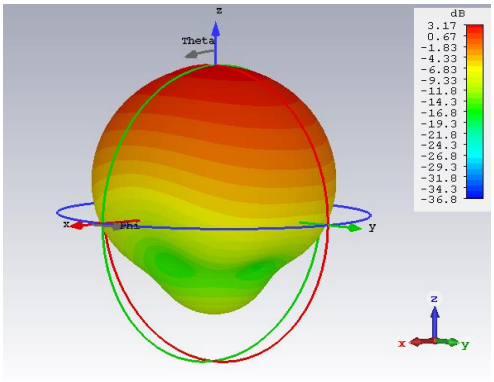

Figure 2.4 Radiation Pattern of MPA.

When representing the radiation pattern, we introduce the E and H-planes which are:

1. E-plane: in the x-z plane (φ = 90°) and is called the elevation plane.

2. H-plane: in the x-y plane (θ = 90°) and is called the azimuth plane.

2.3.8 Polarization

The polarization of an antenna is the polarization of the radiated EM waves produced by an antenna, evaluated in the far field. Polarization of a radiated wave is defined as that property of an EM wave describing the time-varying direction and relative magnitude of the electric-field (E-field) vector. Polarization then is the curve traced by the end point of the vector representing the instantaneous electric field. The field must be observed along the direction of propagation [31]. There exist three polarization types; linear, circular, and elliptical polarization. They are distinguished by looking at the differences in the E-field components.

Co-polarization is the desired polarization of the wave to be radiated by the antenna, that means when the polarization of both the transmitting (test antenna) and receiving antenna (reference horn antenna) is the same. whereas cross-polarization is the orthogonal radiation of the desired polarization of wave, or when the polarization of the two antennas are different.

2.4 Antenna Arrays

An antenna array is a radiating system consisting of "N" spatially separated antennas (starting from two antennas), which are connected using feedlines. The idea behind antenna arrays is to produce more efficient output especially in terms of gain and directivity to meet the demands of the long-distance communications. Antenna arrays can be classified based on the geometry of the overall array (linear, circular, planar or conformal).

2.4.1 Types of Antenna Arrays

a) Linear: linear antenna array consists of N-elements arranged linearly in one direction as depicted in figure 2.5. Linear arrays can be uniform where the phase and amplitude are identical for all elements, or non-uniform where the amplitudes and phases of antenna array of the corresponding elements are unequal [31]. The uniform antenna arrays are the most used and common ones.

The array factor (AF) of the uniform linear array is given by [31]:

$$AF = \sum_{n=1}^{N} e^{j(n-1)\psi} \tag{2.9}$$

Where $\psi = \mathrm{kdcos}\,\theta + \beta$, and can be written in a normalized form by:

$$AF = e^{j\left[\frac{N-1}{2}\right]\psi}\left[\frac{sin\left(\frac{N}{2}\psi\right)}{sin\left(\frac{1}{2}\psi\right)}\right] \tag{2.10}$$

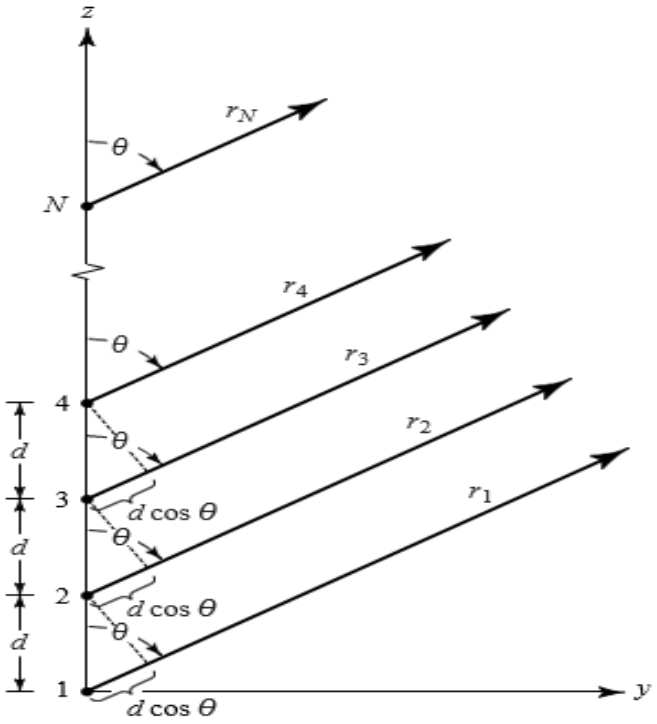

Figure 2.5 Linear Antenna Array.

b) Circular: circular antenna arrays geometry illustrated in figure 2.6, is formed by placing N radiating elements uniformly or non-uniformly on a circle of radius 'a' in 2D plane. It is used in space navigation, Radar and Sonar systems. The array's factor of such structure is given by expression 2.11 [31]:

$$\mathrm{AF}(\theta,\phi) = \sum_{n=1}^{N} I_n e^{jka(\cos\psi - \cos\psi_0)} = \sum_{n=1}^{N} I_n e^{jk\rho_0\cos(\phi_n - \xi)} \tag{2.11}$$

where:

$$\xi = \tan^{-1}\left[\frac{sin\,\theta\,sin\,\phi - sin\,\theta_0\,sin\,\phi_0}{sin\,\theta\,cos\,\phi - sin\,\theta_0\,cos\,\phi_0}\right] \tag{2.12}$$

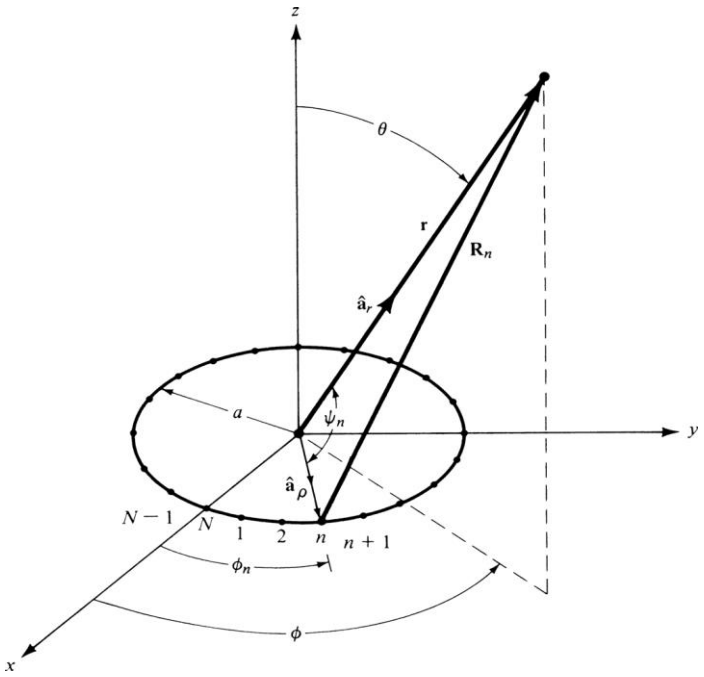

Figure 2.6 Circular Antenna Array.

c) Planar: if we extend the linear antenna array to place the radiating elements along a rectangular grid, then we will form a planar antenna array on two-dimensional plane as shown in figure 2.7:

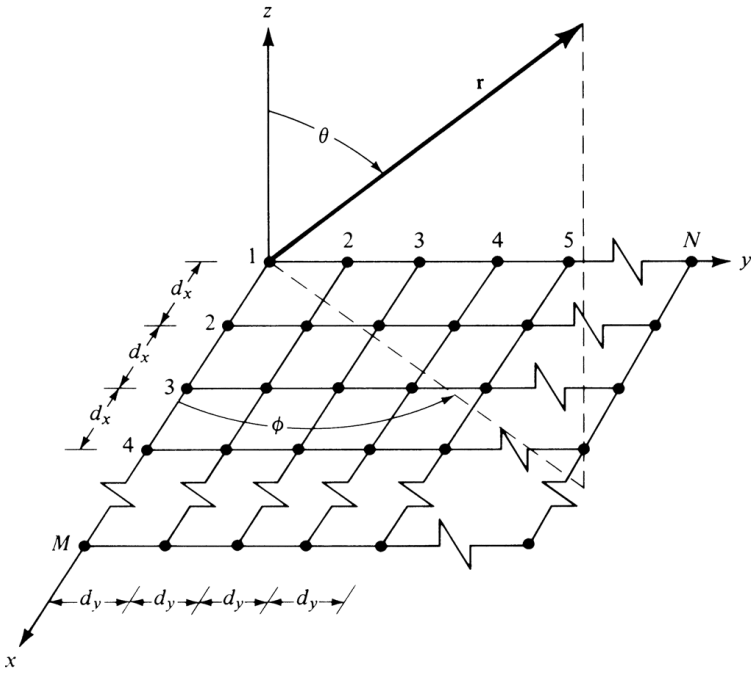

Figure 2.7 Planar Antenna Array.

Planar arrays provide low SLL which is an important factor in WPT applications. Usually planar antenna arrays are designed to fit a rectangular grid (N by M). They are used in tracking

Radar, remote sensing, and other communication applications [37]. The AF for planar arrays can be written as [31]:

$$\mathrm{AF} = \sum_{n=1}^{N} I_{1n}\left[\sum_{m=1}^{M} I_{m1} e^{j(m-1)(kd_x \sin\theta\cos\phi+\beta_x)}\right] e^{j(n-1)(kd_y \sin\theta\sin\phi+\beta_y)} \qquad (2.13)$$

Where d_x, and β_x are the spacing and the progressive phase shift between the elements along the x-axis respectively.

d) Conformal: this type of antenna arrays takes its name from the fact that the radiating elements conform to a pre-defined two-dimensional shape (yet not planar), so they follow a curving object like aircraft surfaces [38]. The conformality to arbitrary shapes makes conformal arrays very useful for ships, submarines, and vehicular communications. Figure 2.8 [39] shows a particular shape of conformal arrays.

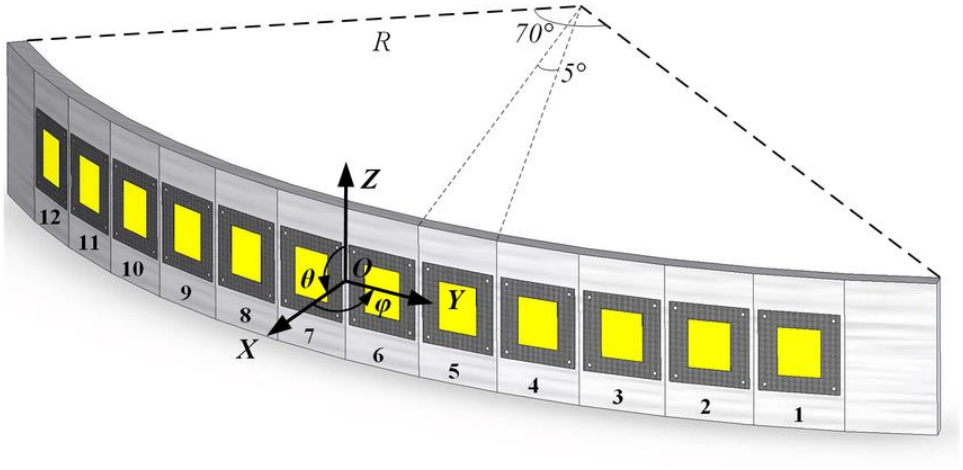

Figure 2.8 Conformal Antenna Array.

2.4.2 Antenna Arrays Feeding

Antenna array's elements are connected by a feeding network which provides power feeding either equally or unequally. The feeding techniques are critical for the overall performance of the antenna array, so a vigilant choice must be taken. Feeding techniques can be series-fed, parallel (corporate feed), or hybrid between the two. Figure 2.9 [40] illustrates antenna array's feeding techniques.

The design of feeding networks is based on power dividers which control the power flow distribution, and split the input signal into two or many output signals to feed the array's elements. The Wilkinson's power divider is the most famous one along with the T-junction power divider.

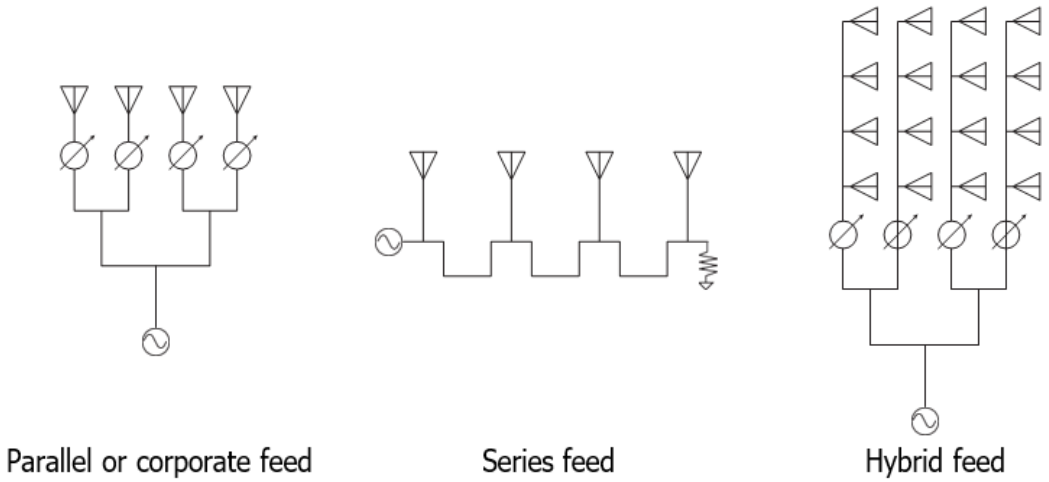

Figure 2.9 Antenna Array's Feeding Techniques.

2.5 Defected Ground Structure

DGS is a compact geometrical slot on the ground plane of a planar transmission line etched periodically or non-periodically [41]. The defects on the ground plane disturb the current distribution leading to a change of characteristics of the corresponding structure, by adding a slot resistance, capacitance, and/or inductance. DGS models are shown in figure 2.10 [42].

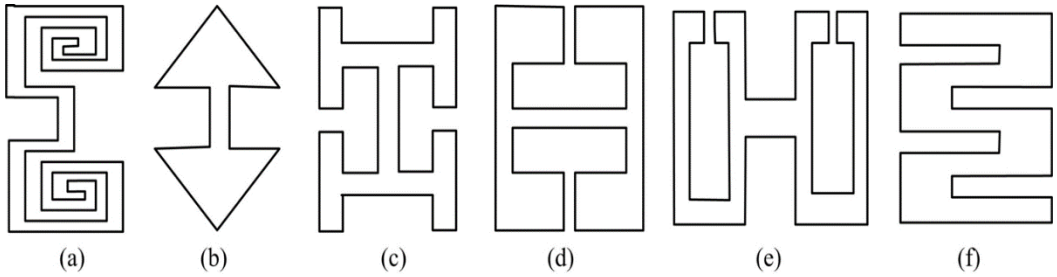

Figure 2.10 Various DGS Models: (a) Spiral Head, (b) Arrowhead-Slot, (c) "H" Shape Slots, (d) A Square Open-Loop with a Slot in Middle Section, (e) Open-Loop Dumbbell (f) Interdigital DGS.

2.6 Parasitic Elements

Parasitic components are placed around the antenna or between the array's elements to reduce the coupling, and to create opposite coupling fields. Parasitic elements do not have their own feeding instead they depend on other's elements feed. They are also not connected to the driven elements such as array's elements. Parasitic component can be used to increase resonance surface of the antenna and the mutual coupling between the patches. There exist two types of parasitic elements: Reflectors, which are made electrically longer than the driven element to reverse the direction of energy emitted from rear of antenna, and Directors which are made shorter than the driven element in order to reinforce and focus energy from the front of the antenna [31].

2.6.1 Electromagnetic Band Gap

Electromagnetic Band Gap (EBG) structures are a special type of periodic parasitic elements. EBG structures are also called high impedance surfaces as they are capable of suppressing surface waves which hinder the performance of MPA array leading to a reduction in the mutual coupling values between the antenna elements [43].

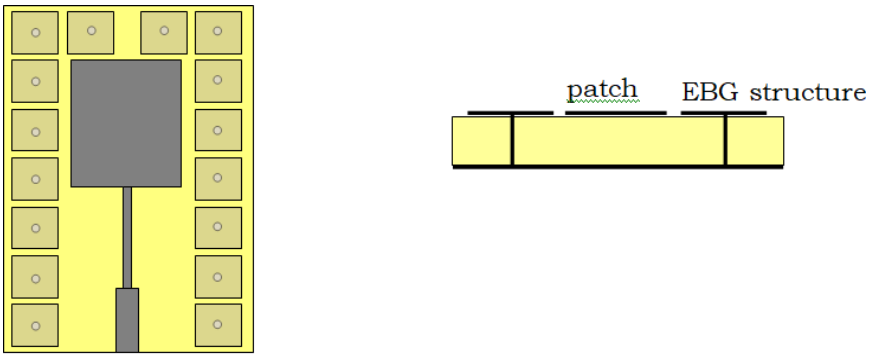

Figure 2.11 Rectangular MPA Surrounded by EBG Structures.

2.6.2 Multilayer Parasitic Element

To overcome the narrow bandwidth and low gain of MPA, researchers have suggested the utilization of multilayer parasitic elements which are based on inserting an air-gap between the radiating patch and a substrate layer with parasitic elements. The air-gap as a dielectric has low permittivity, so it gives an effective radiation pattern and low return loss when it is used as a dielectric substrate between the reflecting and radiating patch [44].

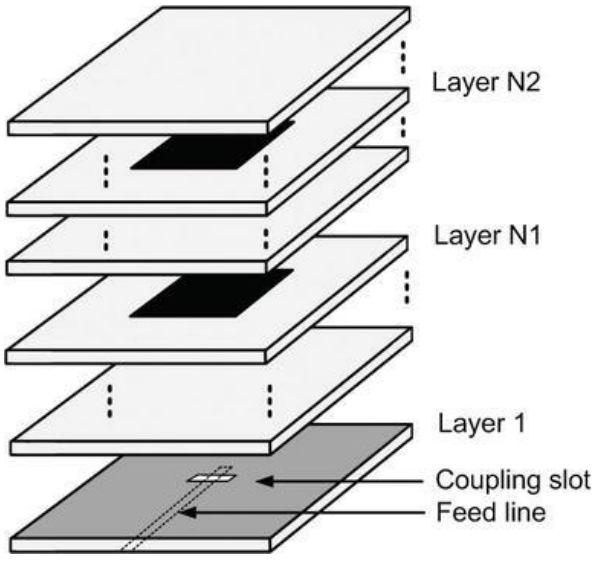

Figure 2.12 Multilayer Parasitic MPA.

2.7 Conclusion

In this chapter, MPAs where introduced along with feeding techniques and methods of analysis which help in the design and analysis of the antenna arrays. Antenna parameters such as gain, return loss, and directivity take a huge amount of interest when analyzing the antenna performance. A good choice and design of the feeding network and defected ground structure model help in enhancing our gain and reflection coefficient. The directivity can be enhanced by placing a large number of antennas together in order to focus the radiated power into the main beam.

Antenna arrays are a key factor for obtaining satisfactory gain and highly directive and narrow beams, so a considerate design along with some modifications are needful to obtain a high gain antenna array with directive main beam, a linear antenna arrays using microstrip patch antenna can be used to meet those requirements.

CHAPTER THREE

Design of Microstrip Antenna Array

3.1 Introduction

For long-distance power transfer, the antenna gain must be large to deliver maximum power to the receiving antenna. Usually, MPA delivers low gain and cannot meet the specifications of the modern power transfer units. To overcome that problem, the designers [55] [19] propose the use of an antenna array so that to enhance the gain, the antenna array also offers an increased directivity augmenting along with the number with the array's elements.

Although an antenna array can reach a considerable gain, it may be in many times not enough for some applications including WPT. For that reason, many enhancements and modifications can be introduced in the design to refine the gain and efficiency. Parasitic elements techniques such as EBG, multilayer parasitic elements, and DGS are commonly used for those reasons. Moreover, an appropriate feeding network for antenna array plays an important role that should be taken into consideration; parallel (or corporate feed) technique is used to power delivery to the array's elements because it is manageable and flexible enough to accommodate modifications in the design.

Several works have been introduced in the last decade related to the design of antenna arrays for applications of WPT. An achievable gain of 7.8 dB and directivity of 10.8 dBi using a 2×2 array, and 10.8 dB gain using a 2×4 array with 14.5 dBi directivity have been obtained in [2] at 2.45 GHz. Other published work [45], has designed an array of 4×1 array with parallel feed achieving a gain of 8.11 dB. Multilayer parasitic elements introduced in [4], where the height and number of layers were incremented at each step to check the difference in gain. While augmenting the height up to a certain limit the gain will increase by a good margin between 1 and 2 dB, after we pass that limit it will decrease eventually. The Dumbbell DGS's shape proposed in [5] is commonly used for its simplicity of design and fabrication. The inset cut feed suggested in [54] is used at the RMPA elements to optimize the performance for varying inset gap and inset length.

In this chapter, an antenna array operating at Wi-Fi 2.45 GHz frequency band with a gain higher than 9 dB and directivity around 12 dBi and based on planar EBG structures, DGS, and multilayer parasitic elements techniques is designed, fabricated, and measured. The substrate is FR-4 which has a relative dielectric constant $\varepsilon_r = 4.3$, thickness of 1.5 mm, and a dielectric loss tangent of 0.017. The design and simulation procedures are carried out using CST microwave studio (MWS) (Appendix A), whereas the fabrication and measurement are made respectively using chemical etching process, and Rohde & Schwarz VNA.

3.2 Design Procedure

3.2.1 Design of the Antenna Array

The first step of this work is based on designing a conventional 2.45 GHz rectangular MPA (RMPA) for its advantages over the other types of radiating patches as mentioned in [53] with inset feed, then two elements of RMPA (antenna array) until we reach the design specifications stated in the previous part.

a) Single Element Antenna: figure 3.1 [31] shows an inset fed RMPA. To calculate the length (L) and width (W) of the RMPA, we use the following equations [48]:

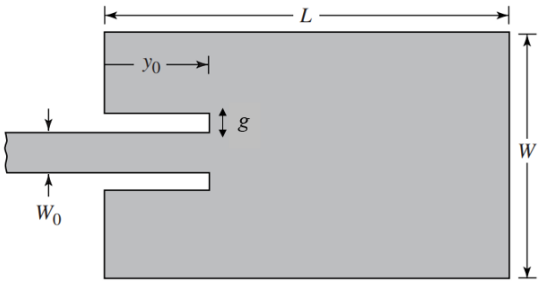

Figure 3.1 RMPA with Inset Feed.

$$W = \frac{c}{2f_0\sqrt{\frac{(\varepsilon_r + 1)}{2}}} \tag{3.1}$$

$$L = \frac{\lambda_0}{f_0\sqrt{\varepsilon_{reff}}} - 2\Delta L \tag{3.2}$$

where ΔL is given by [47]:

$$\Delta L = h \times 0.412 \frac{(\varepsilon_{reff} + 0.3)\left(\frac{w}{h} + 0.264\right)}{(\varepsilon_{reff} - 0.3)\left(\frac{w}{h} + 0.8\right)} \tag{3.3}$$

The inset gap width (g) located at the center of the antenna is taken as a fraction of the microstrip feed line's width, or calculated by equation 3.4 [48]:

$$g = \frac{v_0}{\sqrt{2\times\varepsilon_{eff}}} \frac{4.65\times10^{-12}}{f} \tag{3.4}$$

y_0 is the inset feed point depth which must be located at a point on the patch (radiating edge), where the input impedance is exactly 50 ohms for the resonant frequency [48], we calculate it using:

$$Z_0 = Rin|_{(y=0)}\, cos^2\left(\frac{\pi^* y_0}{L}\right) \tag{3.5}$$

The width of the microstrip feed line W_0 as being illustrated in figure 3.2 is calculated such that the impedance $Z_0 = 50$ ohm using the following equations [13]:

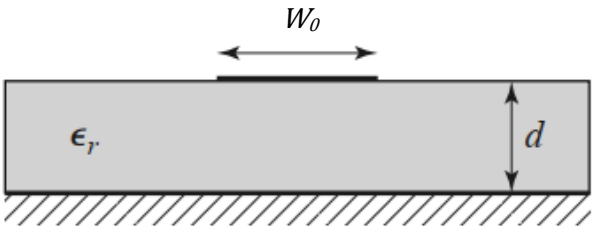

Figure 3.2 Microstrip Feed Line.

$$\frac{W_0}{d} = \begin{cases} \dfrac{8e^A}{e^{2A}-2} & \text{for } W_0/d < 2 \\ \dfrac{2}{\pi}\left[B - 1 - \ln(2B-1) + \dfrac{\epsilon_r - 1}{2\epsilon_r}\left\{\ln(B-1) + 0.39 - \dfrac{0.61}{\epsilon_r}\right\}\right] & \text{for } W_0/d > 2 \end{cases} \tag{3.6}$$

where:

$$A = \frac{Z_0}{60}\sqrt{\frac{\epsilon_r + 1}{2}} + \frac{\epsilon_r - 1}{\epsilon_r + 1}\left(0.23 + \frac{0.11}{\epsilon_r}\right) \tag{3.7}$$

$$B = \frac{377\pi}{2Z_0\sqrt{\epsilon_r}} \tag{3.8}$$

The ground plane is chosen with a removed copper with thickness of 0.035 mm. Its width (W_g) and length (L_g) are taken to be double the width and length of the MPA [46]. The feedline's width is W_0 , and its length is half-wavelength. After calculations we get following results:

Table 3.1 RMPA Dimensions.

parameter	L	W	L_g	W_g	W_0	λ/2	y_0	g
Dimension (mm)	29.10	37.60	58.20	75.22	3.118	29.5	9.50	$W_0/10$

$Rin|_{(y=0)}$ is obtained from [49] and is equal to 238.5 Ohm. After varying the notch width (g), and adjusting the patch length (L) such that the antenna resonates at 2.45 GHz exactly, the following results are obtained:

Table 3.2 RMPA's Simulation Results.

S_{11} (dB)	BW (MHz)	VSWR	Gain (dB)	Directivity (dBi)	SLL (dB)	Efficiency (%)
-26.51	77.88	1.10	3.17	7.05	-12.80	40.96

The patch antenna geometry, and its radiation pattern in polar form illustrating the directivity of the RMPA are shown in Figure 3.3. The antenna's return loss shown in Figures 3.4 shows that the antenna resonates exactly at 2.45 GHz.

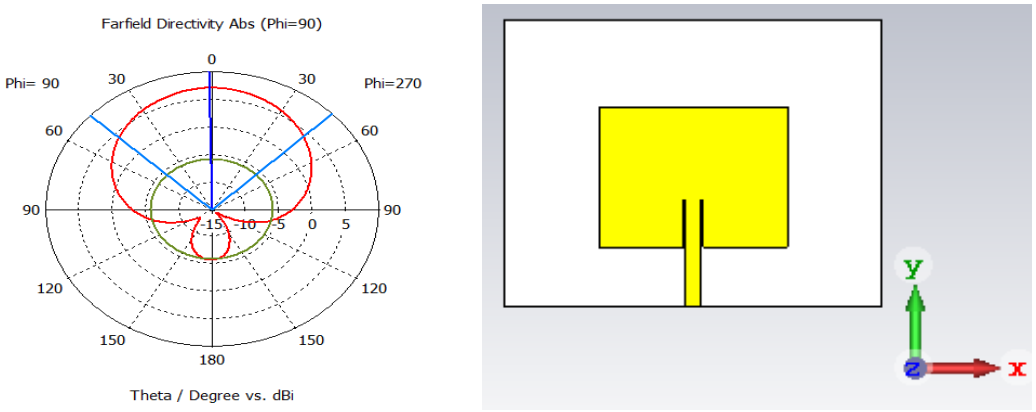

Figure 3.3 Radiation Pattern and the Geometry of Single MPA.

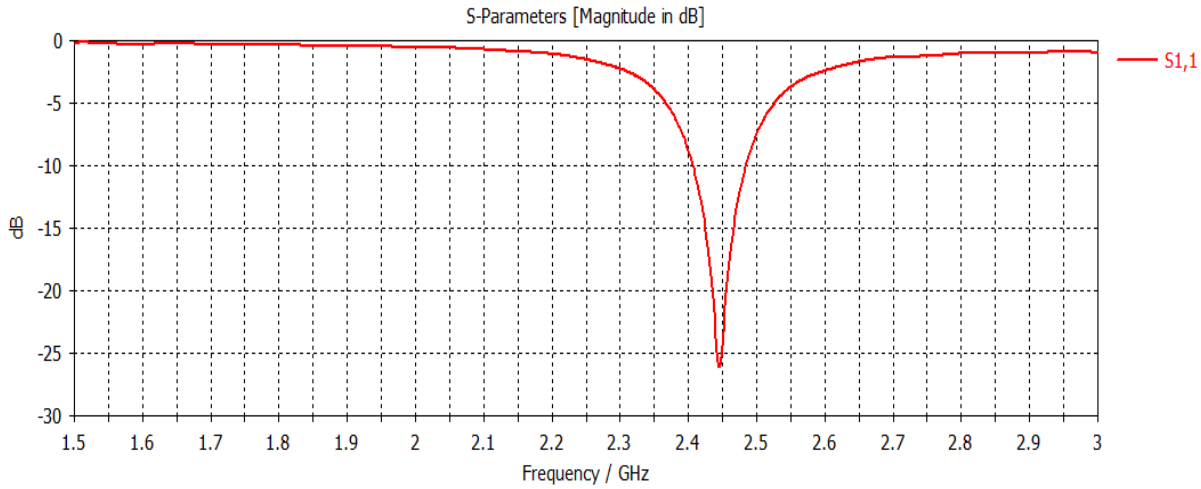

Figure 3.4 Simulated Return Loss of the Single MPA.

One can clearly see that the obtained results are not satisfactory and do not meet our stated goals, so we try with two-elements antenna array.

b) Two-elements MPA array: To design the two-elements antenna array, we have to design first a parallel feeding network such that it splits the power equally to the two RMPAs. That can be done by 50 Ohm feed line divided into two parallel 100 Ohm feed lines. The width of 100 Ohm feed lines (L_1) is calculated using equation (3.6), where the length of 100 Ohm feed line (W_1) is $\lambda_g = 59.18\ mm$. Figures 3.5 and 3.6 show the feeding network with its dimensions (in millimeters), and the two-elements antenna array's geometry and its 3D radiation pattern respectively:

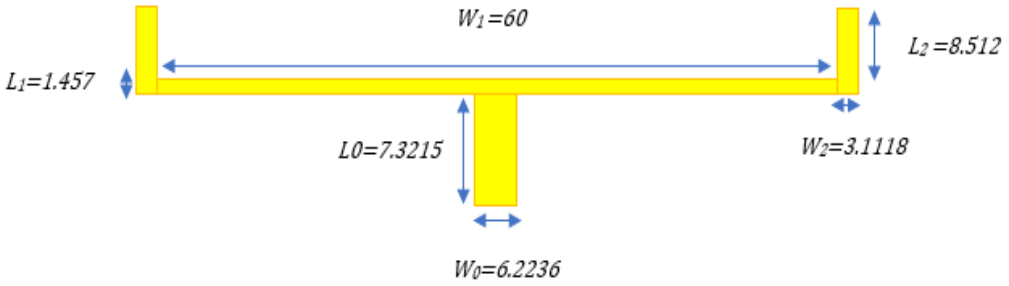

Figure 3.5 Feed Network for a Two-elements Microstrip Antenna Array.

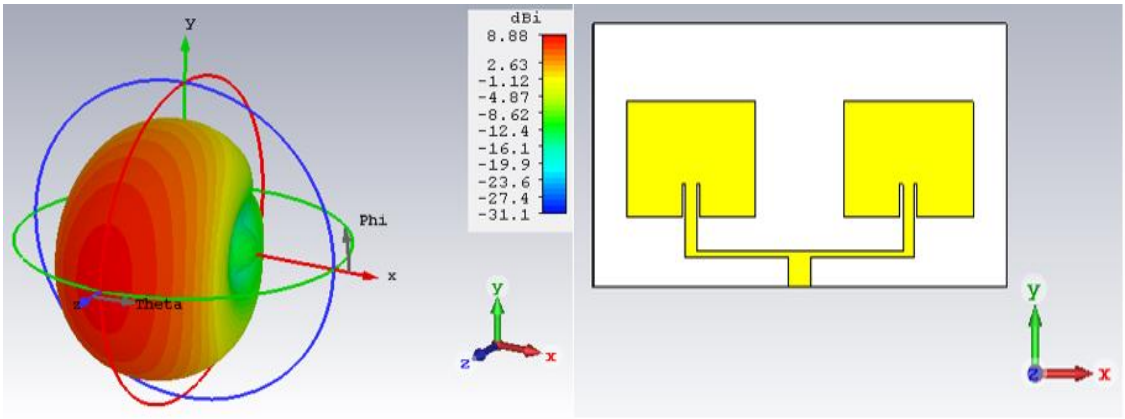

Figure 3.6 Geometry of Two-elements Antenna Array along with its Radiation Pattern.

After performing parametric study on the width and the length of the feeding lines we have found the results shown in the table below. The two-elements antenna array did not reach the desired goals and hence will be upgraded to four-elements antenna array. The gain and directivity did not change significantly but the antenna array is well matched giving a return loss less than -29 dB at 2.45 GHz as shown in figure 3.7:

Table 3.3 Simulated Results of the Two-elements Antenna Array.

S_{11} (dB)	BW (MHz)	VSWR	Gain (dB)	Directivity (dBi)	SLL (dB)	Efficiency (%)
-29.18	109.06	1.08	5.62	8.88	-13.40	47.30

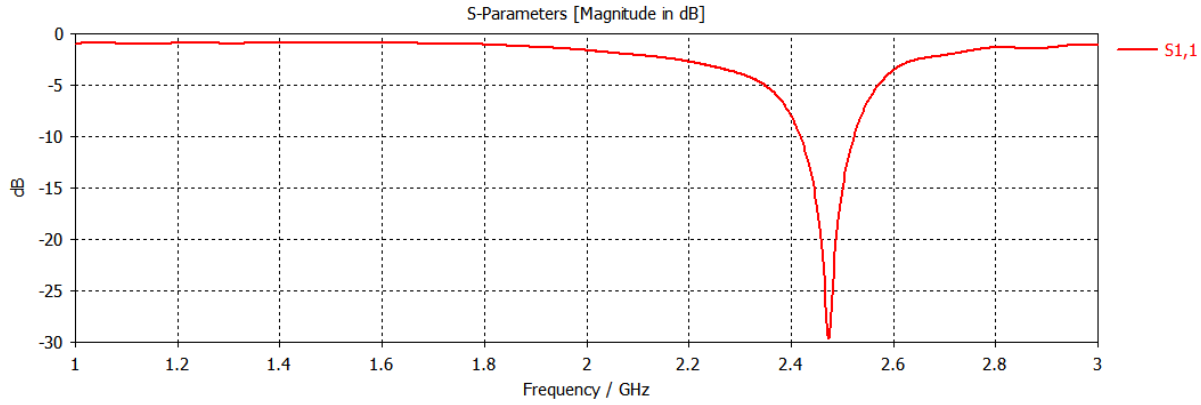

Figure 3.7 Simulated Return Loss of the Two-elements Antenna Array.

c) Four-elements MPA array: as we did before, we start by designing the feeding network for the four-elements antenna array using the corporate feed technique. We can track the power flow of the feeding network in CST's 2D/3D results to help us modify the design to minimize power losses. The dimensions of the feeding network illustrated in Figure 3.8 are given in table 3.4:

Table 3.4 Dimensions of the Four-elements Feeding network.

parameter	W_0	L_0	W_1	L_1	W_2	L_2	W_3	L_3	W_4	W_5
Dimension (mm)	6.2236	7.3215	110	1.457	3.118	8.514	55	7.3	58.118	51.888

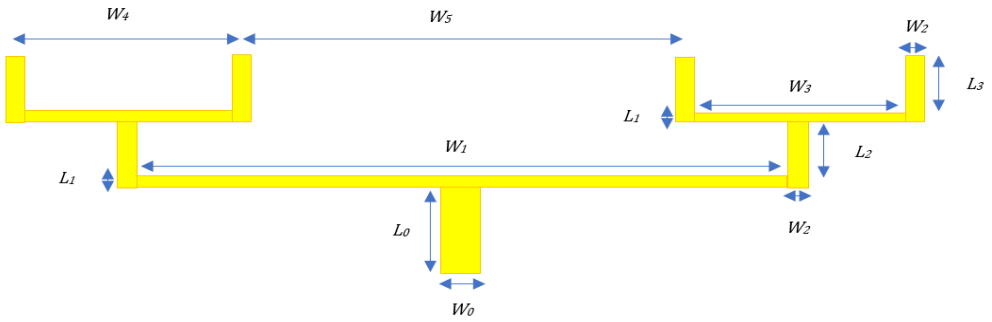

Figure 3.8 Feeding Network for Four-elements Antenna Array.

After simulation, we obtained the results shown in Table 3.5. One can see that the gain did not reach the desired value but the directivity became high. Another remark is that the return loss is decreased and it is not sufficient. Hence, by using CST's integrated optimizer (Appendix A) and adding the metered bend shapes at the corners and junctions of the feeding network to decrease S_{11} and eliminate the distortion in reflection coefficient [57] as shown in Figure 3.9.

Table 3.5 Simulated Results of Four-elements Antenna Array.

S_{11} (dB)	BW (MHz)	VSWR	Gain (dB)	Directivity (dBi)	SLL (dB)	Efficiency (%)
-13.68	74.52	1.52	7.80	11.90	-15.90	40.03

The modified antenna array's results are given in table 3.6 (The patch dimensions after the bends where used are: W = 37.6099 mm, L = 27.9 mm). With radiation pattern and return loss shown in figures 3.10, and 3.11 respectively.

Table 3.6 Simulated Results of the Modified Four-elements Antenna Array.

S_{11} (dB)	BW (MHz)	VSWR	Gain (dB)	Directivity (dBi)	SLL (dB)	Efficiency (%)
-31.96	141.32	1.05	7.92	11.80	-15.70	41.00

Figure 3.10 shows that the directivity of the antenna array has a maximum value of 11.80 dBi at 2.45 GHz in the direction of z-axis, which is close to the desired goal.

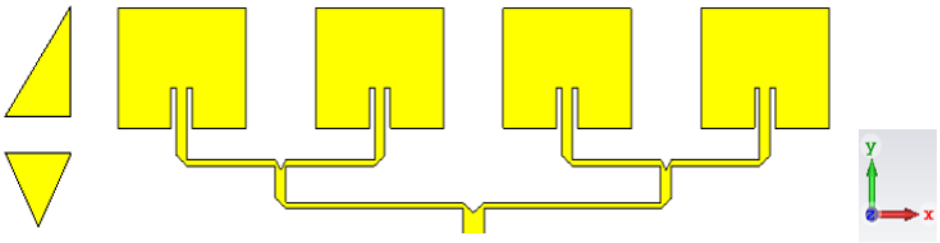

Figure 3.9 Modified Four-elements Antenna Array after Introducing Bends.

The radiation pattern:

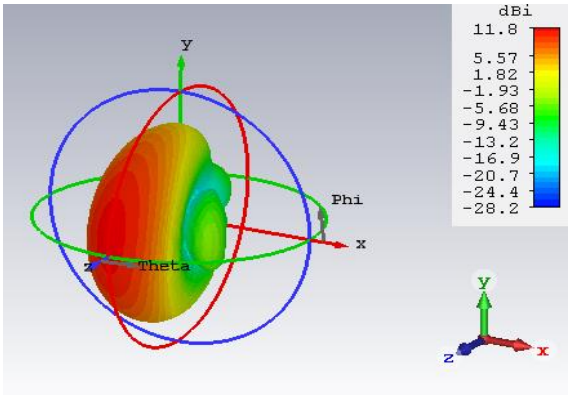

Figure 3.10 Radiation Pattern of the Modified Antenna Array.

The return loss (S_{11}):

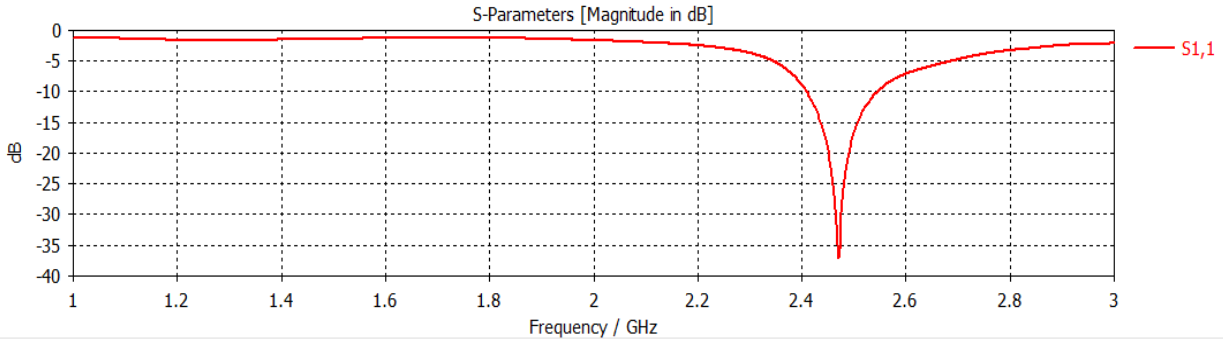

Figure 3.11 Simulated Return Loss of the Modified Antenna Array.

For further improvements, we vary the inset gap width (g) and fix the other parameters (feeding network dimensions, the patch length L and width W, and the inset length y_0) as suggested in [54], to spot the difference in the antenna array parameters. Table 3.7 displays the obtained results. We have also changed the notch length (y_0), but the results were not satisfactory. Where the gain decreased and the antenna resonance frequency shifts to 2.68 GHz. Other parameters are well set.

Table 3.7 Comparison between Different Notch Widths.

Notch width (g)	$W_0/2$	$W_0/4$	$W_0/6$	$W_0/8$	$W_0/10$
S_{11} (dB)	-16.00	-31.96	-20.20	-23.60	-16.72
VSWR	1.40	1.05	1.23	1.30	1.68
Gain (dB)	7.61	7.92	7.70	7.89	7.62
Directivity (dBi)	11.80	11.80	11.60	11.80	11.40
SLL (dB)	-14.70	-15.70	-14.50	-13.90	-12.40
BW (MHz)	95.23	141.32	124.73	125.70	120.00
Efficiency (%)	38.20	41.00	41.60	40.00	41.00

Although the gain did not reach 9 dB value, but we can optimize it using the techniques stated before. Hence, we stop at four-elements antenna array and start to improve it. So that brings us to the end of the primary design, next we will optimize the four-elements MPA array.

3.2.2 Performance Improvement of the Antenna Array

As we have mentioned before, we stopped at four-elements antenna array and now we try to enhance it using the techniques we discussed in chapter two. The basic structure we chose is the four radiating elements shown in figure 3.9, since it gave the best results compared to other designs. The first step is to design the four elements antenna array with DGS. Then, with EBG, and finally combining them together.

a) Using DGS: we have chosen the well-known DGS shape proposed in [5], called the Dumbbell. We place it between the radiating elements vertically. Figure 3.12 depicts the Dumbbell:

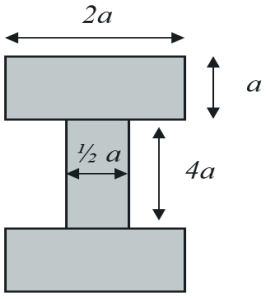

Figure 3.12 Proposed DGS's Shape: The Dumbbell.

The width (a) of the shape will be varied and compared when we put it between each two radiating elements making it total of three DGS shapes as shown in figure 3.13 (a). And when putting five DGS shapes as figure 3.13 (b) shows, then we compare our results. The shapes are

aligned vertically because when we have tried placing the structures horizontally the return loss is less than -10 dB and the VSWR is greater than 2, so we only consider the vertical aligning.

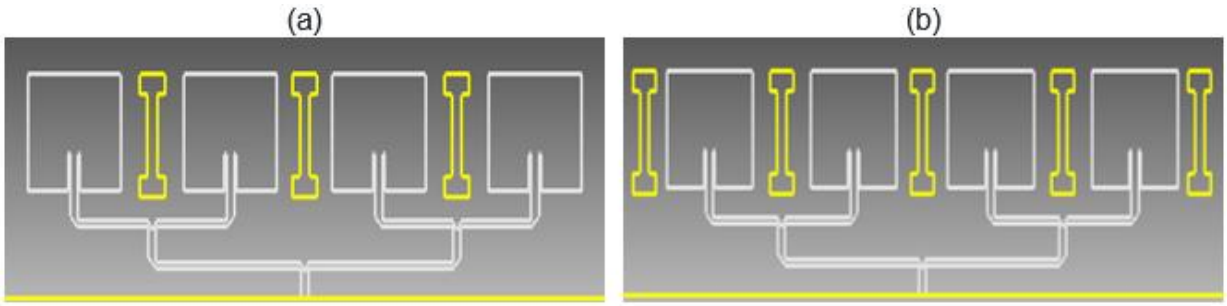

Figure 3.13 Dumbbell DGS: (a) 3 Elements DGS, (b) 5 Elements DGS.

Table 3.8 Comparison between the DGS's Elements' Width.

position	3 DGS's elements			5 DGS's elements		
Width 'a' (mm)	4	5	6	4	5	6
S_{11} (dB)	-26.60	-30.69	-24.3	-26.60	-30.55	-24.20
VSWR	1.29	1.13	1.31	1.19	1.15	1.23
Gain (dB)	7.94	7.98	7.90	7.94	7.98	7.85
Directivity (dBi)	11.80	11.80	11.60	11.80	11.80	11.60
SLL (dB)	-15.20	-15.80	-15.20	-15.30	-15.80	-14.80
BW (MHz)	192.92	247.31	185.70	195.90	246.50	185.90
Efficiency (%)	41.60	42.80	41.80	41.60	42.80	41.80

From the table above, we can see that the results are quite far from our goals, since the gain increased slightly by 0.06 dB which is not enough. The vertical positioning of the DGS gave the best results in both the three and five DGS elements, specifically when the width is 5mm we have got approximately the same results. From that, we can say that the number of DGS elements do not change the results significantly, hence we keep the three DGS elements for further designs. Furthermore, from figure 3.14 which shows the current distribution of the antenna array with DGS (a), and without DGS (b); one can see clearly that the current distribution of the antenna array with DGS is concentrated at the center of the RMPAs rather than the edges and the feedlines. Whereas in (b) where the antenna array is left without DGS shapes, the current distribution is spread through the RMPA's edges and corners along with the feedlines. Hence, DGS helps in redistributing the antenna current such that it is concentrated at the center of RMPAs.

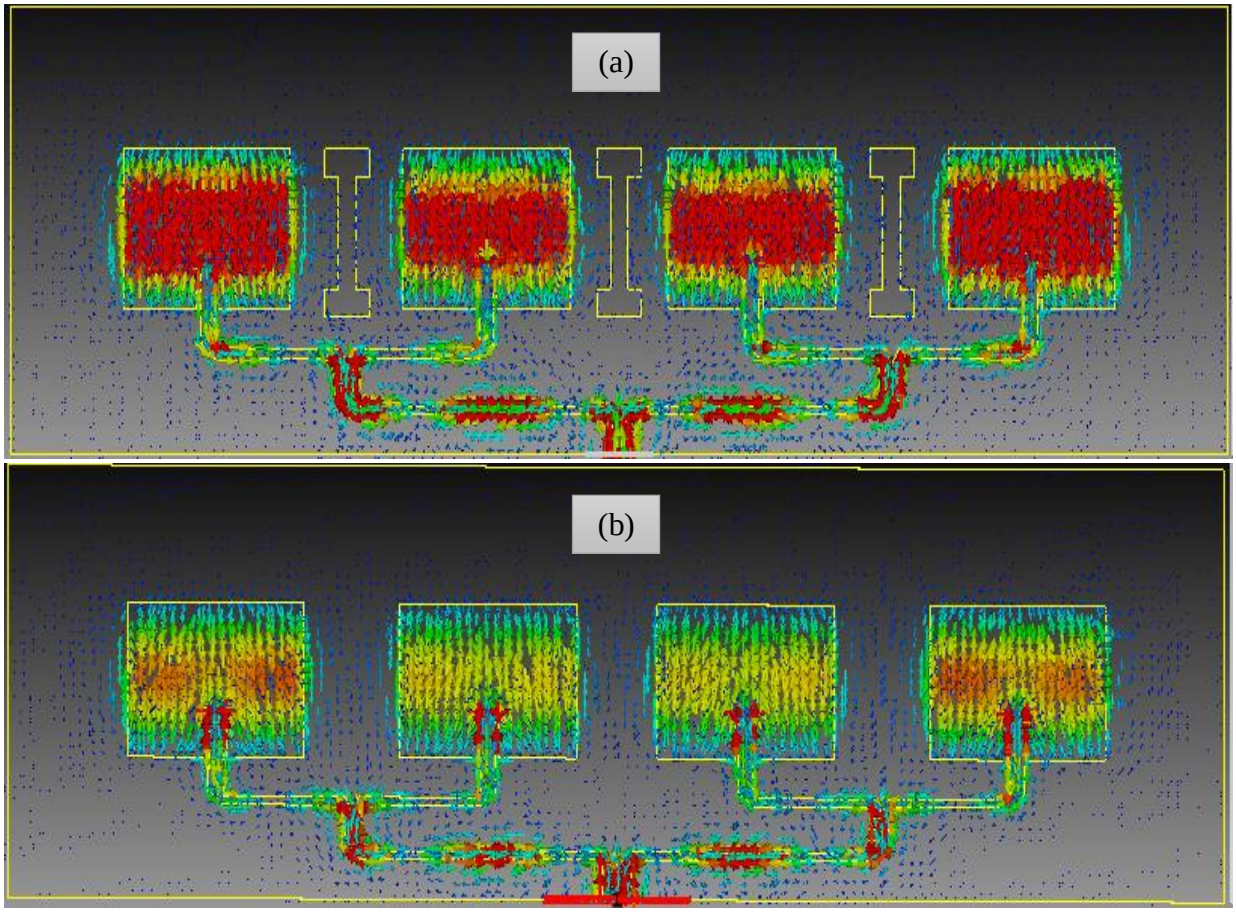

Figure 3.14 Current Distribution of the Antenna Array: (a) With DGS, (b) Without DGS.

b) Using EBG: the EBG is usually placed around the patch from above, left and right. There are many shapes and structures that can be used. In our case we choose two shapes (b) [3], and (c) [5], and another one we design it ourselves (a), as illustrated in figure 3.15. The EBG shapes are designed one at each time, to see which shape gives the best gain and directivity. After that the number of EBG's elements is also changed. The results are shown in table 3.9 below:

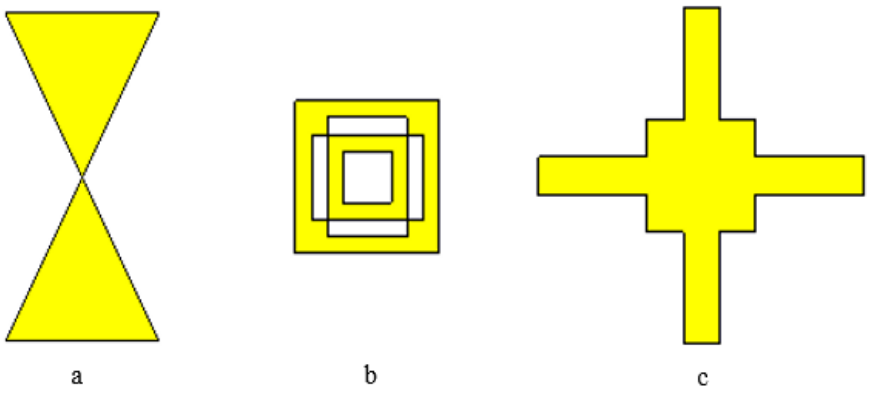

Figure 3.15 EBG Shapes: (a) First Shape, (b) Second shape, (c) Third shape.

Table 3.9 Comparison between EBG's Shapes Number.

shapes	Shape one (a)		Shape two (b)		Shape three (c)	
Number of elements	15	30	15	30	15	30
S_{11} (dB)	-29.70	-25.84	-23.27	-23.45	-26.95	-26.76
VSWR	1.12	1.11	1.14	1.14	1.09	1.11
Gain (dB)	7.98	7.95	7.85	8.03	8.09	8.08
Directivity (dBi)	12.10	12.10	11.80	11.80	12.10	12.10
SLL (dB)	-14.20	-14.40	-13.70	-14.20	-14.60	-14.60
BW (MHz)	135.77	122.89	142.00	158.00	148.23	155.50
Efficiency (%)	43.40	43.00	43.40	45.00	46.40	46.40

We can see from the results in table 3.9, that the third shape illustrated in Figure 3.15 (c) gave the best results approximately in all parameters. Furthermore, the number of EBG's elements did not change the gain or any other parameter except for the bandwidth. From now on we select the shape in figure 3.15 (c), and try to change the design such that we get the best result out of it. The number of elements is fixed to be 24 elements arranged in different positions around the antenna array's radiating elements as shown in figure 3.17. The dimensions of the EBG are also changed in order to increase the resonance surface of it, figure 3.16 depicts the final shape of the EBG with its dimensions:

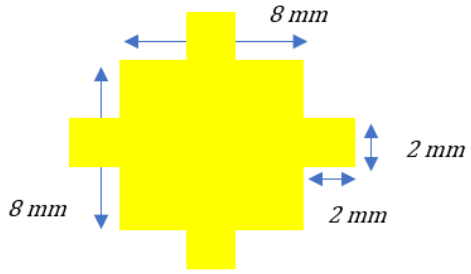

Figure 3.16 Final EBG Shape with its Dimensions.

From the results shown in table 3.10, we can see that the position (a) where we used three groups of six elements between each two consecutive radiating elements and six elements in the top of the array, gave the best results. Our aim of obtaining directivity larger than 12 dBi is accomplished but the gain is always less than 9 dB. Neither the DGS nor the EBG techniques were able to lead us to that target, so we combine them together.

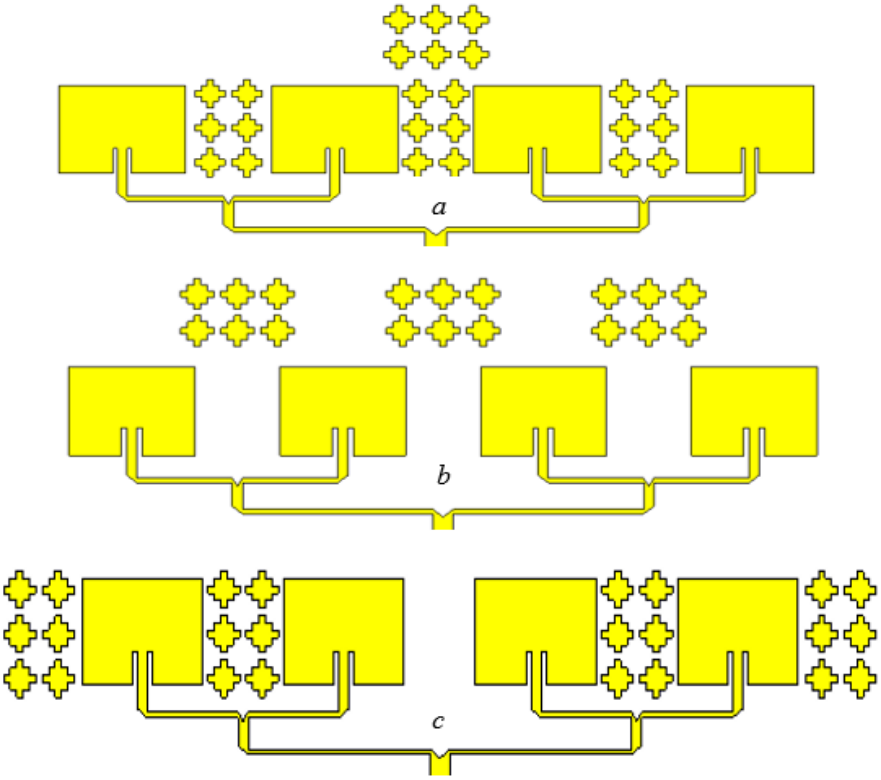

Figure 3.17 Different EBG Positions Around the Antenna Array.

Table 3.10 Comparison between Different EBG's Positions.

positions	a	b	c
S_{11} (dB)	-28.28	-24.54	-27.90
VSWR	1.08	1.12	1.08
Gain (dB)	8.22	8.14	8.16
Directivity (dBi)	12.10	12.10	12.10
SLL (dB)	-15.20	-14.40	-14.90
BW (MHz)	137.50	143.63	115.98
Efficiency (%)	40.70	40.10	40.20

c) Using EBG + DGS: the DGS Dumbbell shape placed vertically between each two array's elements is combined with the EBG shape shown in figure 3.16, as illustrated in figure 3.18 below.

Table 3.11 Simulated Results of the EBG and DGS Combination.

S_{11} (dB)	BW (MHz)	VSWR	Gain (dB)	Directivity (dBi)	SLL (dB)	Efficiency (%)
-27.32	183.49	1.08	8.32	12.10	-15.6	41.30

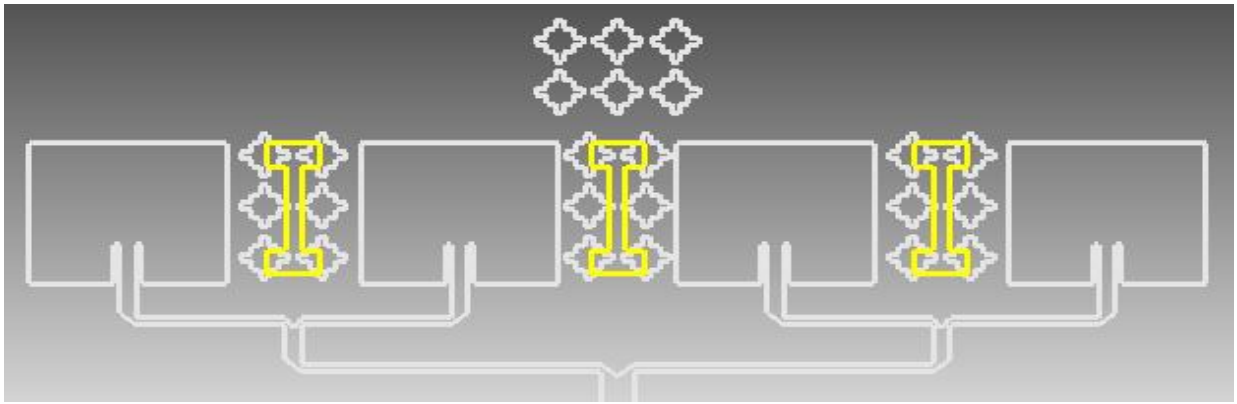

Figure 3.18 Antenna Array Containing DGS and EBG.

From the table 3.11 above, we can see that the gain has increased slightly which tends to be a much lower value from our goal. The SLL also is under -20 dB and in that case, we have large losses of the power in the side lobes. It is clear that the EBG and the DGS techniques alone cannot fulfill our objectives of high gain and low SLL, hence the multilayer parasitic elements technique is used next.

d) Using multilayer parasitic elements: After we did not reach our objectives in the last sections. We use the multilayer technique now. In order to do that, the starting point is the design shown in Figure 3.18 having the following dimensions:

Table 3.12 Four-elements Antenna Array Dimensions.

parameter	W_0	L_0	W_1	L_1	W_2	L_2	W_3	L_3
Dimension (mm)	6.3364	7.3215	120	1.55	3.1702	8.513	60	7.3
parameter	W_4	W_5	g	y_0	L	W	L_g	W_g
Dimension (mm)	58.118	51.888	$W_0/3$	8.4	30	37.61	100	280

Based on the paper [4], the additional layer must contain rectangular parasitic elements on the top of the antenna array. We suggest the addition of triangles on the top of the rectangular parasitic elements. The parasitic elements improve the gain since they increase the resonance surface of the antenna. Many layers can be used, but we must also take into consideration the space it will take and the fabrication difficulties coming from that. In our work we design multilayer antenna array of maximum three layers. Figure 3.19 shows the layer which we used in our design with its dimensions, containing four triangular and rectangular parasitic elements

combined together. The layer will be on the top of the antenna array and separated by an air-gap from it.

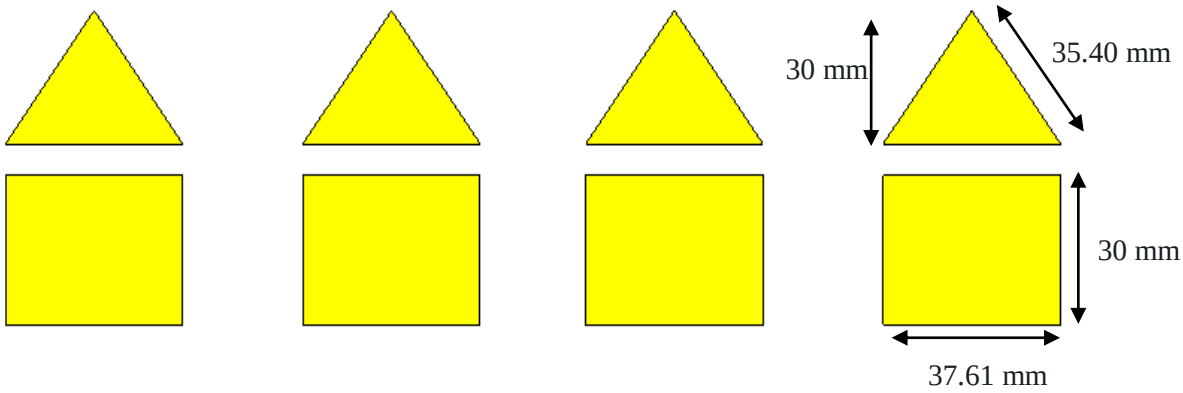

Figure 3.19 The Proposed Multilayer Parasitic Elements.

First: we start by one layer, the distance between it and the antenna array is varied and the results are displayed in the table 3.13. The air-gap increases the thickness of the substrate hence enhancing the gain without increasing the substrate's height. However, the results may go in the wrong direction if we increment the air-gap's height indefinitely. For that reason, we start by 5 mm in height (lower values decreased the already achieved gain), then we increase it up to where it is no longer improving the antenna array's parameters.

Table 3.13 Comparison between Different Heights of the One Parasitic Layer.

Height (mm)	5.4	6.4	7.4
S_{11} (dB)	-22.97	-37.94	-20.79
VSWR	1.15	1.03	1.20
Gain (dB)	10.30	10.90	10.80
Directivity (dBi)	12.70	13.30	13.10
SLL (dB)	-21.00	-20.30	-20.90
BW (MHz)	325.65	180.53	256.53
Efficiency (%)	57.55	53.40	60.6

The single layer enabled us to reach the gain threshold we set in the start of the project. It also provided an SLL less than -20 dB with a directivity of 13.10 dBi which is more than what we targeted at the start. The bandwidth which is an important factor of the antenna reaches 180 MHz. The return loss was below -30 dB with a VSWR of nearly 1, so our antenna array is well matched.

Second: now we add another layer to the layer we designed before and go through the same process of varying the air-gap's height. The results are shown in the table below:

Table 3.14 Comparison between Different Heights of the Two Parasitic Layers.

Height (mm)	5.4	6.4	7.4
S_{11} (dB)	-20.76	-22.37	-18.23
VSWR	1.22	1.16	1.28
Gain (dB)	10.30	10.40	10.40
Directivity (dBi)	13.10	13.30	13.40
SLL (dB)	-16.20	-15.90	-13.90
BW (MHz)	268.29	261.14	453.92
Efficiency (%)	55.60	51.50	50.50

As table 3.14 shows, the two multilayer parasites did not increase the gain nor it did decrease the SLL. At 7.4 mm height, the directivity reaches 13.40 dBi which is the highest value obtained till now, and the bandwidth also passed 450 MHz making it a great choice for the applications requiring large bandwidth.

Third: now we try three layers combined at the same time to check if the gain increases. The table below shows the obtained results from the simulations:

Table 3.15 Comparison between Different Heights of the Three Parasitic Layers.

Height (mm)	5.4	6.4	7.4
S_{11} (dB)	-18.60	-16.20	-15.17
VSWR	1.44	1.56	1.56
Gain (dB)	9.65	9.88	9.97
Directivity (dBi)	13.50	13.50	13.50
SLL (dB)	-13.10	-13.10	-13.10
BW (MHz)	282.56	277.27	283.41
Efficiency (%)	44.30	45.00	45.00

The first, second, and third layers designs are illustrated in figure 3.20. We did not get any enhanced gain from the three multilayer parasitic array antennas, but the directivity reached 13.50 dBi. Next, we will compare the best result which is highlighted in green in table 3.13 (a) with the four elements antenna array without EBG and DGS (b), with DGS only (c), and with EBG only (d), by adding single layer of parasitic elements to them to compare by how much the multilayer did improve the antenna parameters.

Table 3.16 Comparison between Different Designs.

The design	a	b	c	d
S_{11} (dB)	-37.94	-18.58	-19.80	-19.01
VSWR	1.03	1.26	1.26	1.28
Gain (dB)	10.90	9.70	9.80	10.00
Directivity (dBi)	13.30	12.70	13.00	13.00
SLL (dB)	-20.30	-18.00	-19.20	-19.00
BW (MHz)	180.53	254.22	232.72	228.88
Efficiency (%)	53.40	54.80	52.50	53.00

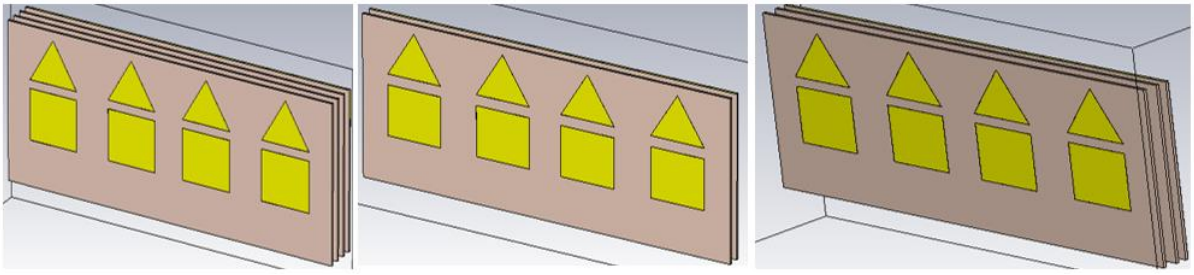

(a) (b) (c)

Figure 3.20 Different Antenna Array Designs of Multilayer Parasitic Elements: (a) Three Layers, (b) One Layer, (c) Two Layers.

The single layer antenna array highlighted in green in table 3.16 is the best among all the designs we have seen so far. Hence, we choose it as our final design since it fulfills all our requirements that we have fixed at the start of our project. In order to fabricate the antenna array, we need to make sure that the antenna array's input impedance Z_{in} is equal to the feeding port which has an impedance of 50 Ohm. The simulated input impedance of the antenna array is approximately 50 Ohm around 2.45 GHz frequency, as shown in figure 3.21:

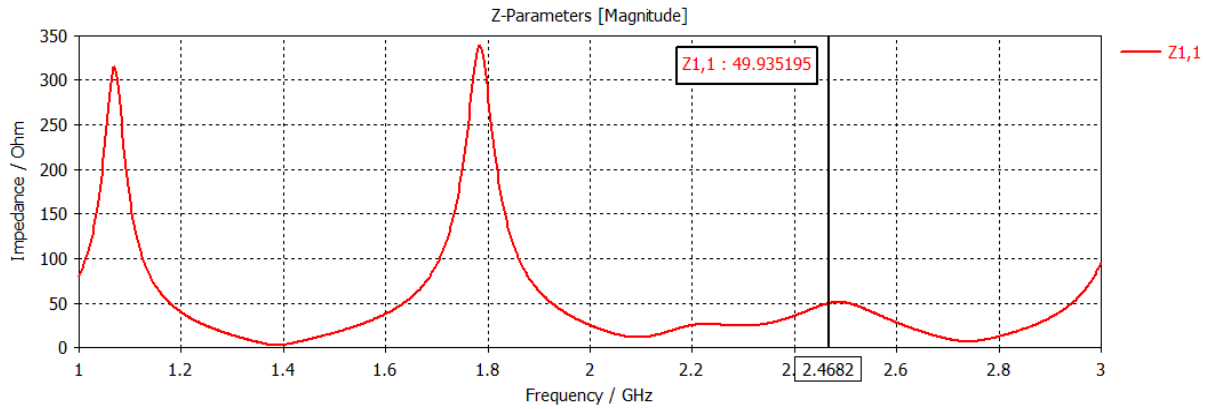

Figure 3.21 Simulated Input Impedance of the Antenna Array.

From Figure 3.24, the gain is above 10 dB in the range from 2.2 to 2.6 GHz, giving a stable and steady performance all over the bandwidth of 180 MHz (our BW ranges from 2.36 GHz to 2.54 GHz). Figure 3.22 illustrates the radiation pattern of the antenna array; the maximum directivity is 13.30 dBi at the resonance frequency with side lobes less than -8.00 dBi for an SLL less than -20 dB. The current's distribution of the antenna array shown in figure 3.23, is mainly concentrated at the center of the four RMPAs and throughout the feedlines, and is minimized at the corners.

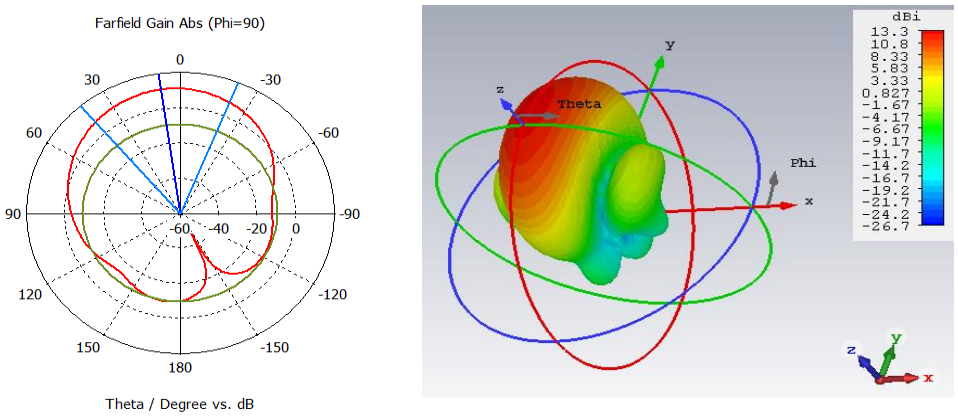

Figure 3.22 Radiation Pattern of the Antenna Array in Polar and 3D Forms .

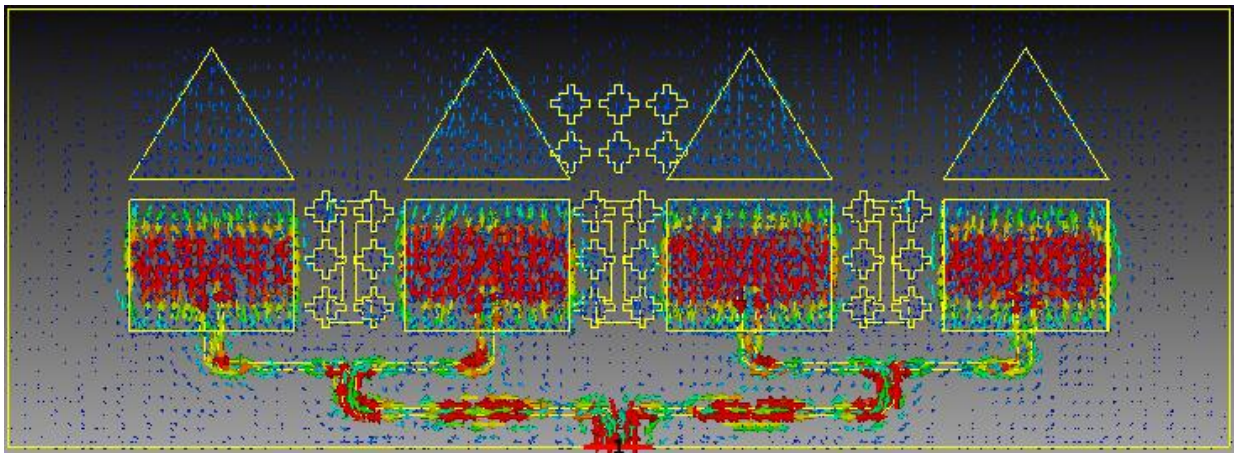

Figure 3.23 Current Distribution of the Antenna Array.

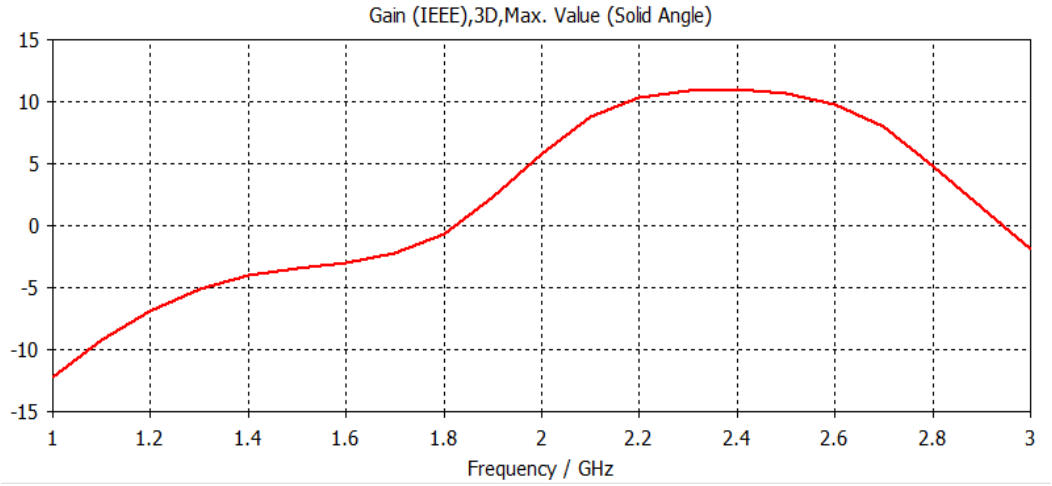

Figure 3.24 Simulated Gain versus Frequency of the Antenna Array.

The polarization of the antenna arrays is also an important factor for harmonizing the transmission and reception of the antennas. The axial ratio (AR) of an antenna determines the polarization's type, values between 0 to 3 dB refer to circular polarization, AR values between 3 to 10 dB refer to elliptical polarization, whereas linear polarization corresponds to AR's values greater than 10 dB. In our case the polarization of the antenna array is linear based on the axial ration (AR) displayed in figure 3.25, giving a value of 20 dB around the resonance frequency:

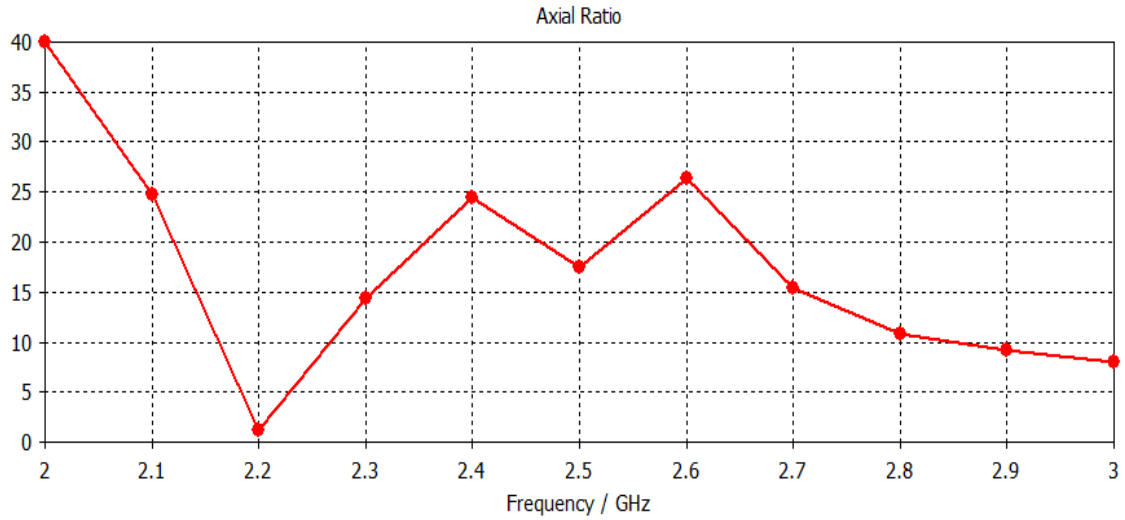

Figure 3.25 Simulated Axial Ratio of the Antenna Array.

The co-polarization corresponding to the desired polarization of the antenna array must be greater by 20 dB than the cross polarization, which is the orthogonal polarization of the desired one in both E and H-planes. Figures 3.26 and 3.27 show the polar radiation pattern of the antenna array in E-planes and H-plane respectively.

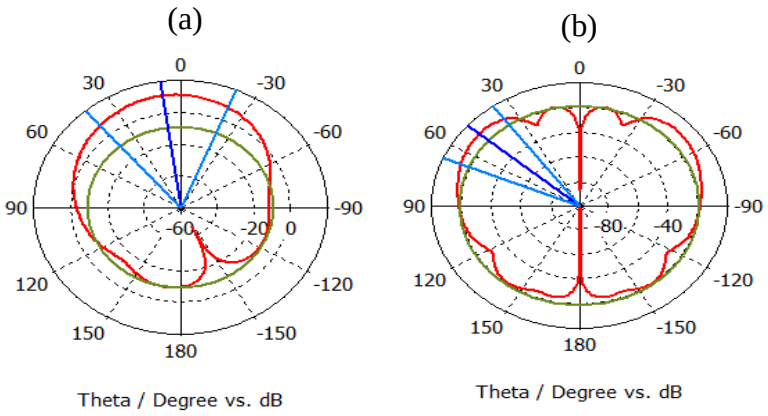

Figure 3.26 E-Plane Radiation Pattern: (a) Co-Polarization, (b) Cross Polarization.

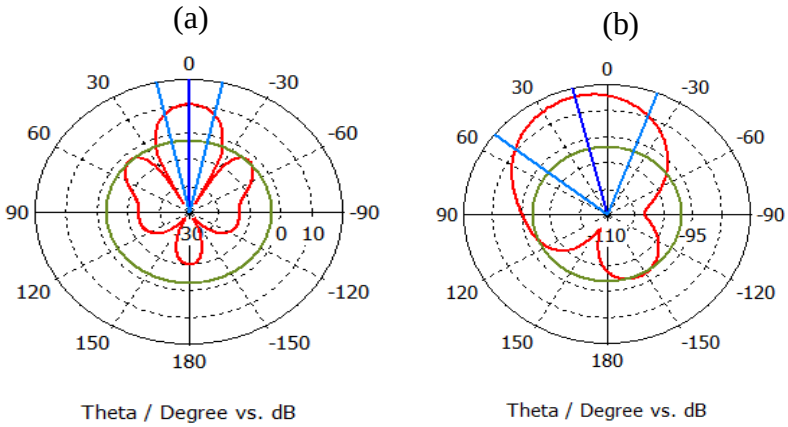

Figure 3.27 H-Plane Radiation Pattern: (a) Co-Polarization, (b) Cross Polarization.

The main lobe of the co-polarization in the E-plane shows a value of 10.9 dB while the main lobe of the cross polarization in the E-plane has a value of -9.54 dB. Moreover, the main lobes in the H-plane has value of 10.6 dB in co-polarization, and -85.4 dB in the cross polarization. Hence, we have a good polarization purity since the difference is more than 20 dB between the co and cross polarization in both E and H-planes.

Another point of interest when dealing with WPT, is the ability of the antenna array to handle maximum power transfer. The power capacity P_{max} , is estimated computationally according to the square relationship between power and field intensity as [1] :

$$P_{max} = \left(\frac{E_{br}}{E_0}\right)^2 P_{in} \tag{3.9}$$

Where P_{in} is fixed to 1 Watt in CST, it is used to calculate the maximum E-field intensity. E_0 is the maximum electrical field intensity as shown in figure 3.28, and E_{br} is the vacuum breakdown threshold (6.4 MV/m in the S band [52]).

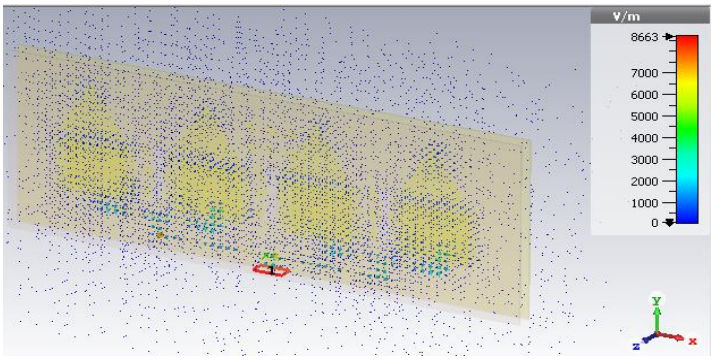

Figure 3.28 Electric Field Intensity of the Antenna Array.

From the figure we can see that the maximum electric field intensity is 8663 V/m. Hence, the power capacity obtained by equation (3.9) is 574.787 KW which is the theoretical value, actually the real value is much less than that. However, it is still a reasonable value for WPT.

3.3 Fabrication and Experimental Results

The proposed antenna array based on EBG, DGS, and parasitic layer is fabricated in a laboratory outside of our institute and this is due to lack of material means (such as substrate and PCB etching process for large surfaces ”chemical etching process”) is shown in figures 3.29 and 3.30:

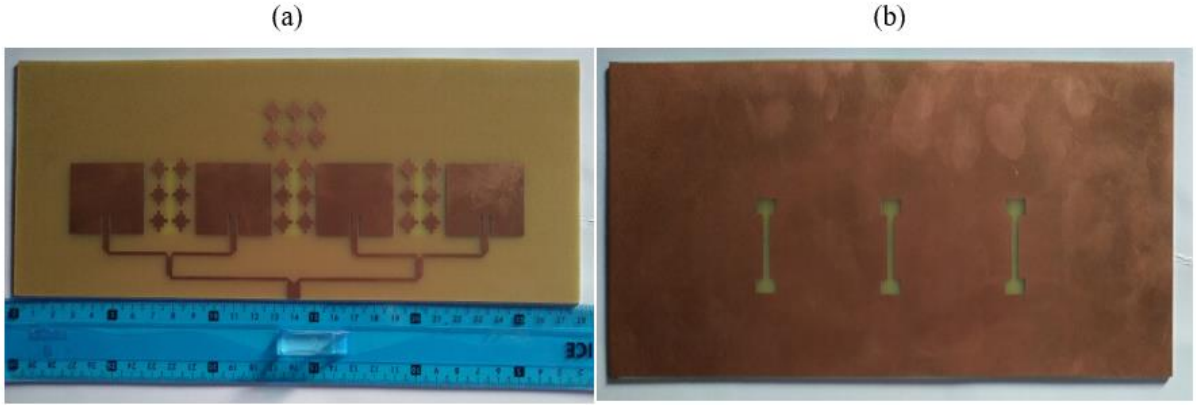

Figure 3.29 Photography of the Antenna Array; (a) Top View, (b) Back View

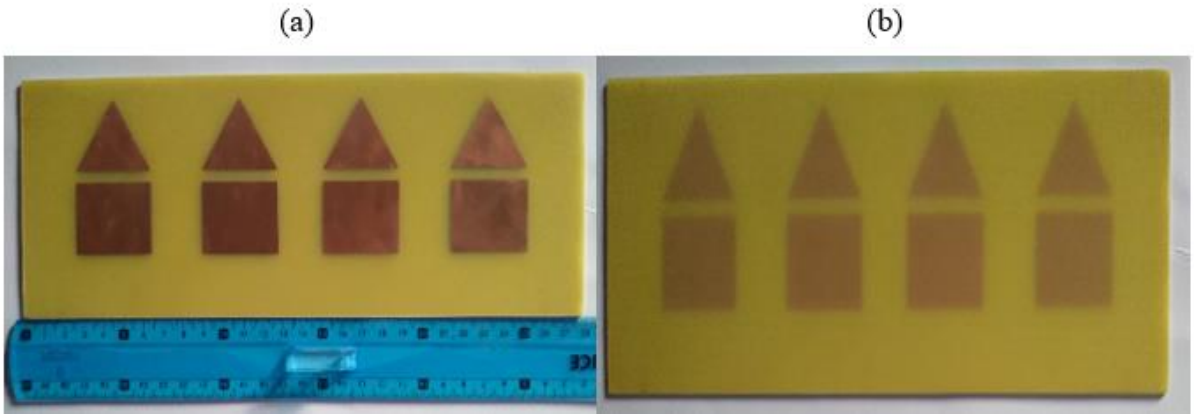

Figure 3.30 Photography of the Parasitic Layer; (a) Top View, (b) Back View.

The parasitic layer is connected to the antenna array by means of four plastic supports placed in each corner of the antenna array, as shown in figure 3.31:

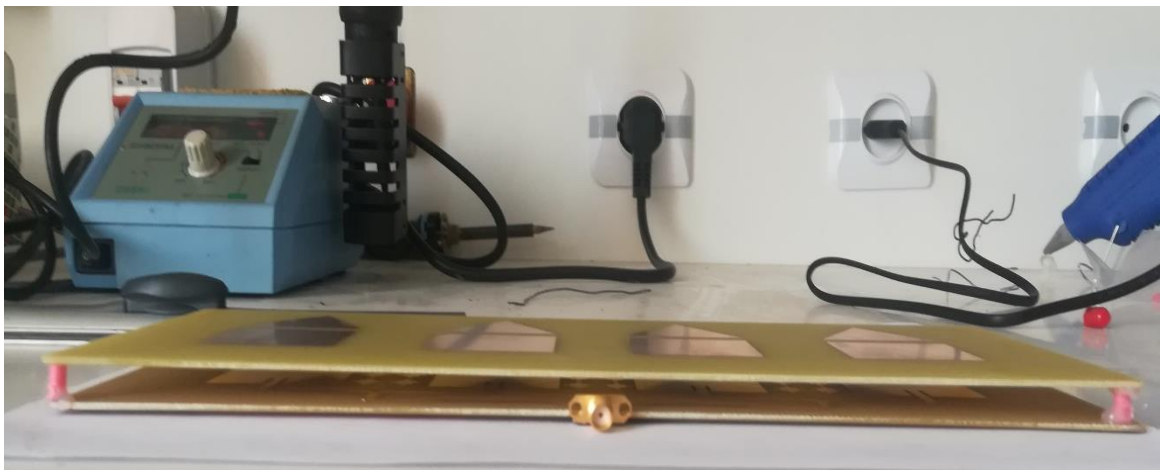

Figure 3.31 Final Prototype of the Proposed Antenna Array.

The simulate and measured S_{11} magnitude in dB of the proposed antenna array is shown in figure 3.32. There is a good level of agreement between simulated and measured results. A degradation in the return loss is most probably attributed to the tolerance and soldering in the fabrication process, diversity of material parameters and additional insertion loss of SMA connectors.

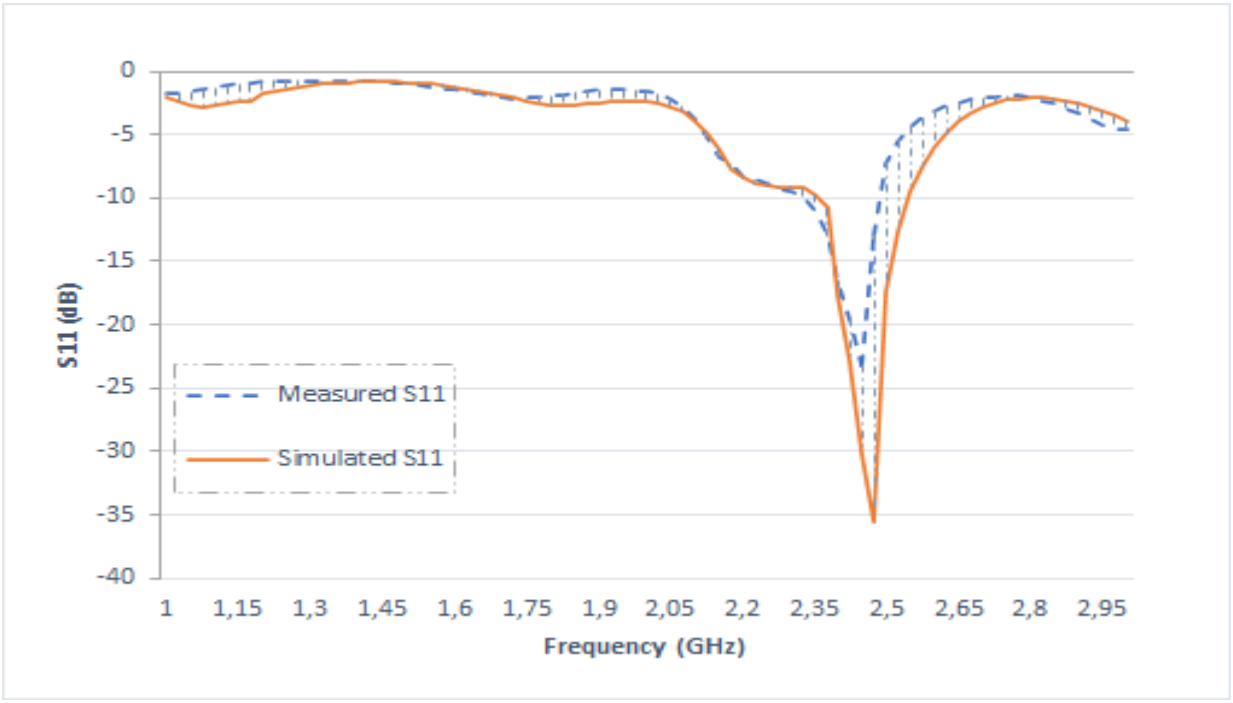

Figure 3.32 Simulated and Measured S_{11} of the Proposed Antenna Array.

In order to see how well is our array antenna design and performance, we compare it with previous works which operate also at 2.45 GHz. Table 3.17 provides comparison of our antenna

array with other works. It is apparent that the proposed antenna array has the widest bandwidth and the highest antenna gain and directivity, with nearly similar SLL and return loss values. Although that the work presented in [1] uses 16 antenna elements with more sophisticated materials (PTFE spacers and Aluminum), we still have got close values especially in SLL and directivity. The work presented in [2] is also for WPT, we can see that for the same number of array elements and the same substrate material, we achieved good performance. This result makes the proposed design very suitable to be utilized for a WPT system.

Table 3.17 Performance Comparison of the Proposed Antenna Array with other Reported Works.

Reference	current work	[1]	[2]	[3]	[4]
Application	WPT	WPT	WPT	Long way communication system	4G LTE antenna
Materials	FR-4	Aluminum, PTFE spacers	FR-4	FR-4	FR-4
Size (mm)	280*100	2280*600	122*128	118*175	151.5*151.5
Number of Elements	4 elements	16 elements	4 elements	4 elements	2 elements
S_{11} (dB)	-37.94	-30.00	-24.20	-34.32	-21.72
Directivity (dBi)	13.30	14.00	10.80	8.30	-
Gain (dB)	10.90	13.00	7.80	7.00	8.29
SLL (dB)	-20.30	-20.00	-21.90	-	-
Bandwidth (MHz)	180.53	400.00	76.50	80.00	48.00
Efficiency (%)	53.40	75-90	-	-	-

3.4 Conclusion

In this chapter, a new type of long-range antenna array for WPT applications operating at 2.45 GHz have been designed, fabricated, and measured. The proposed antenna array at the resonant frequency has a maximum gain of 10.90 dB, and a directivity of 13.30 dBi with peak-to-side lobe level suppression of -20.30 dB. The bandwidth is around 180 MHz, the return loss is less than -37 dB, and the VSWR nearly equals unity so we can say safely that the antenna array is well matched, hence minimizing the power losses. The antenna efficiency is around 53 %.

GENERAL CONCLUSION

Within this work, a breakthrough long-range WPT has been introduced for WSNs utilizations, along with a general review about antenna arrays theory and parameters. Microstrip patch antenna are usually used for WPT applications for their advantages over other antenna types. Since MPAs offer low gain and efficiency which obstruct the required performance of the antenna array, efficient techniques like EBG and multilayer parasitic elements can be used in order to improve the performance of the antenna array to meet the desired specification.

Four-elements linear antenna array of dimensions 280 mm × 100 mm has been designed, fabricated and measured to be utilized at the Tx side of a long-range WPT system. The antenna array operates at the Wi-Fi 2.45 GHz frequency and covers a bandwidth of 180 MHz from 2.36 to 2.54 GHz. Multilayer parasitic elements, EBG, and DGS techniques were used to enhance the antenna array parameters such as gain and directivity. The proposed antenna array is fed through a corporate feeding network. The antenna array shows a good performance with a stable gain of 10 dB in the antenna array bandwidth, and of 10.90 dB at the resonant frequency 2.45 GHz. The directivity of the antenna array reaches 13.30 dBi with SLL value of -20.3 dB. The reflection coefficient amplitude is less than -35 dB (VSWR < 1.03). The power handling capability is nearly 545 KW which makes the proposed antenna array an excellent candidate for a long-range WPT system with multiple rectennas.

The suggested future work on this subject is:

- Using more sophisticated materials, like crystal and aluminum in order to increase the gain and the overall efficiency.
- Steering the antenna array's main beam from 0° to 90°, using frequency phase shifters.
- Increasing the array's elements up to 16 radiating elements, to augment the power handling of the array from Kilowatts to Megawatts.

REFERENCES

[1] A. M . Eid, A. Alieldin, A. M. El-Akhdar, A. F. El-Agamy, W. M. Saad, A. A. Salama, 2021. "A novel high-power frequency beam-steering antenna array for long-range wireless power transfer". In 2021 Alexandria Engineering Journal, 60(2), pp.2707-2714.

[2] G. B. Hoang, G. N. Van, L. T. Phuong, T. A. Vu, and D. B. Gia, 2016, October. “Research, design and fabrication of 2.45 GHz microstrip patch antenna arrays for close-range wireless power transmission systems”. In 2016 International Conference on Advanced Technologies for Communications (ATC) (pp. 259-263). IEEE.

[3] L. Shital, D. Vaishali, 2017. “Microstrip antenna array without and with square EBG structure”. In 2017 International journal of Engineering Sciences & Research Technology.

[4] A. B. Santiko, K. Paramayudha, Y. Wahyu and H. Wijanto, 2016, July. “Design and realization multilayer parasitic for gain enhancement of microstrip patch antenna”. In 2016 International Seminar on Intelligent Technology and Its Applications (ISITIA) (pp. 299-304). IEEE.

[5] K. P. Rao, R. M. Vani and P. V. Hunagund, 2018. “Planar microstrip patch antenna array with gain enhancement”. In 2018 Procedia computer science, 143, pp.48-57.

[6] M. Rashid, "Power Electronics Handbook,"- ISBN: 978-0-12-811407-0 - Copyright © 2018 Elsevier Inc. All rights reserved.

[7] M. W. Basnayaka, Chathuranga. "Wireless Energy Transmission for AccessLimited Underground Sensors". University of Ruhuna. Retrieved 8 May 2020.

[8] R. Erfani, F. Marefat, A. M. Sodagar and P. Mohseni, 2017, May. “Transcutaneous capacitive wireless power transfer (C-WPT) for biomedical implants”. In 2017 IEEE International Symposium on Circuits and Systems (ISCAS) (pp. 1-4). IEEE.

[9] M. Etemadrezaei, "Power Electronics Handbook, 4th Edition," -ISBN 978-0-128-11407-0- Copyright © 2017, Butterworth-Heinemann.

[10] S. S. Mohammed, K. Ramasamy and T. Shanmuganantham, 2010. “Wireless power transmission–a next generation power transmission system”. In 2010 International Journal of Computer Applications, 1(13), pp.100-103.

REFERENCES

[11] ITU-International telecommunication Union: Recommendation ITU-R "Nomenclature of the Frequency and Wavelength Bands used in Telecommunications" (ITU Legal Affairs Unit - Table 1 reproduction permission, Hebrew translation, July 25, 2014).

[12] Guru, Bhag Singh, Hüseyin R. Hızıroğlu (2004). "Electromagnetic Field Theory fundamentals, 2nd Edition". Cambridge Univ. Press. pp. 422–423. ISBN 978-1139451925.

[13] D. M. Pozar, "Microwave Engineering, Fourth edition," -ISBN 978-0-470-63155-3- copyright © 2012, 2005, 1998 by John Wiley & Sons, Inc. All rights reserved.

[14] J. Stiles, "A Comparison of Common Transmission Lines and Waveguides," Foundations of Interconnect and Microstrip Design, Third Edition, 2009.

[15] K. C. Gupta, R. Garg, I. J. Bahl and P. Bhartia, "Microstrip Lines and Slot lines," Artech House, Boston, 1996.

[16] S. M. Palhade and S.P. Yawale. 2015. "Design and photo-lithographic fabrication of microstrip patch antenna". Int. J. Sci. Res, 4(2), p.2021.

[17] C. Robinson, T. Piwtorak and B. Souid, "Synthesis and Analysis of Microstrip and Stripline Transmission Line Structures," Syracuse University, Project Report, 2011.

[18] S. W. Ellingson, "Electromagnetics 1, Handbook" Virginia Technology University.

[19] S. Wadkar, B. Hogade, R. Chopra and G. Kumar, 2019. "Broadband and high gain stacked microstrip antenna array". In 2019 Microwave and Optical Technology Letters, 61(7), pp.1882-1888.

[20] I. Rosu, "Microstrip, Stripline, and CPW Design," RF Technical Articles, Bucharest, Romania, 2012.

[21] Matthew N. O. Sadiku, "Elements of Electromagnetics," ISBN 978-0-195-13477-3- Copyright © 2000 Oxford University Press.

[22] Jia-Sheng hong M. J. Lancaster, "Microstrip Filters for RF/Microwave Applications," -ISBN 0-471-22161-9- Copyright © 2001 by John Wiley & Sons.

[23] M. J. Gao, L. S. Wu and J. F. Mao, 2012 "Compact notched ultra-wideband bandpass filter with improved out-of-band performance using quasi-electromagnetic bandgap structure," In 2012 Progress In Electromagnetics Research, vol. 125, pp. 137-150.

REFERENCES

[24] C. Nguyen, "Analysis Methods for RF, Microwave, and Millimeter-Wave Planar Transmission Line Structures," New York: John Wiley & Sons, 2003

[25] S. Belomestnykh, "Transmission lines and S-parameters, Lecture 1 - RF fundamentals for mechanical engineers," U.S. Department of Energy - Office of Science, Brookhaven National Laboratory, 2011.

[26] S. J. Orfanidis, "Electromagnetic Waves and Antennas," -ISBN 978-0-13-093855-8- Copyright © 2003 by Prentice Hall.

[27] G. Marconi,11 December 1909. "Wireless Telegraphic Communication". Nobel Lecture. Archived from the original on 4 May 2007."Physics 1901–1921". Nobel Lectures. Amsterdam: Elsevier Publishing Company. 1967. pp. 196–222, 206.

[28] I. Singh and Tripathi, V.S., 2011. "Microstrip patch antenna and its applications: a survey". In 2011 Int. J. Comp. Tech. Appl, 2(5), pp.1595-1599.

[29] G. A. Deschamps, "Microstrip microwave antennas", 3rd USAF Symposium on Antennas, 1953.

[30] K. F. Lee, K. M. Luk, "Microstrip Patch Antennas", -ISBN -13 978-1-84816-453-6- Copyright © 2011 by Imperial College Press.

[31] C. A. Balanis, "Antenna Theory: Analysis and Design, 4th Edition," ISBN: 978-1-118-64206-1- Copyright © 2016 by John Wiley & Sons, Inc.

[32] S. Bisht, S. Saini, V. Prakash and B. Nautiyal, 2014. "Study the various feeding techniques of microstrip antenna using design and simulation using CST microwave studio". In 2014 International Journal of Emerging Technology and Advanced Engineering, 4(9), pp.318-324.

[33] V. Palanisamy and R. Garg, 1986. "Analysis of arbitrarily shaped microstrip patch antennas using segmentation technique and cavity model". In 1986 IEEE Transactions on Antennas and Propagation, 34(10), pp.1208-1213.

[34] R. B. Waterhouse, "Microstrip Patch Antennas: A Designer's Guide," -ISBN 978-1-4757-3791-2- Copyright © 2003 by Springer Science+Business Media New York

[35] T. S. Bird, 2009. "Definition and misuse of return loss". In 2009 IEEE Antennas and Propagation Magazine, 51(2), pp.166-167.

[36] http://wireless.ictp.it/handbook/C4.pdf

[37] S. H. Hsu, Y. J. Ren and K. Chang, 2009. “A dual-polarized planar-array antenna for S-band and X-band airborne applications”. In 2009 IEEE Antennas and Propagation Magazine, 51(4), pp.70-78.

[38] Josefsson, P. Persson, L. Josefsson, P. Persson, 2006. "Conformal array antenna theory and design". In 2006 USA: John Wiley and Sons. pp. 1–9. ISBN 0-471-46584-4.

[39] J. Zhang, H. Kang, N. Hu, Y. Chen, J. Huang, Y. Qin, S. Zha and X. Huang, 2019, June. “Structural Mutual Coupling Calibration Experiments of Full Polarization Conformal Phased Array”. In 2019 Joint International Symposium on Electromagnetic Compatibility, Sapporo and Asia-Pacific International Symposium on Electromagnetic Compatibility (EMC Sapporo/APEMC) (pp. 700-703). IEEE.

[40] S. V. Hum, "Radio and Microwave Wireless Systems," Page 17, ECE422.

[41] H. Louazene, M. Challal and M. Boulakrouneb, 2015 "Compact Ultra-Wide Band Bandpass Filter Design Employing Multiple-Mode Resonator and Defected Ground Structure," In 2015 Procedia Computer Science Journal, vol. 73, pp. 376-383.

[42] L. H. Weng, Y. C. Guo, X. W. Shi and X. Q. Chen, 2008. “An overview on defected ground structure”. In 2008 Progress In Electromagnetics Research, 7, pp.173-189.

[43] K. P. Rao, R. M. Vaniand P. V. Hunagund, 2018. “Planar microstrip patch antenna array with gain enhancement”. In 2018 Procedia computer science, 143, pp.48-57.

[44] K. W. S. Al Kharusi, N. Ramli, S. Khan, M. T. Ali and M. A. Halim, 2020. “Gain enhancement of rectangular microstrip patch antenna using air gap at 2.4 GHz”. In 2020 International Journal of Nanoelectronics and Materials, 13(Specia), pp.211-22

[45] P. M. Masud, 2013. "A methodology for designing 2.45 GHz wireless rectenna system utilizing Dickson Charge Pump with Optimized Power Efficiency (Master's thesis, University of Waterloo)"

[46] G. V. P. Pranathi, N. D. Rani, M. Satyanarayana, G. T. Rao, 2015. “Patch antenna parameters variation with ground plane dimensions”. In 2015 Int J Adv Res Electric Electronics Instr Eng, 4, pp.2320-3765.

[47] T. A. Milligan, "Modern Antenna Design," McGraw-Hill Book Co., New York, 1985.

REFERENCES

[48] M. A. Matin, A. I. Sayeed, A.I., 2010. "A design rule for inset-fed rectangular microstrip patch antenna". In 2010 WSEAS Transactions on Communications, 9(1), pp.63-72.

[49] http://www.emtalk.com/mpacalc.php

[50] E. T. Aye and C. M. Nwe, 2014. “Rectangular microstrip patch antenna array for RFID application using 2.45 GHz frequency range”. In 2014 Int. J. Sci. Res, 4(6), pp.1-2.

[51] G. A. Vandenbosch, A. Vasylchenko, 2011. “A practical guide to 3D electromagnetic software tools”. In 2011 INTECH Open Access Publisher.

[52] A. Semnani, A. Venkatraman, A. Alexeenko, D. Peroulis, 2013. “Frequency response of atmospheric pressure gas breakdown in micro/nanogaps”, In 2013 Appl. Phys. Lett. 103063102 (2013).

[53] Nasir, Jamal. (2016). Re: What is Co-Polarization and Cross-Polarization in terms of both E-Plane and H-Plane in HFSS?. Retrieved fromhttps://www.researchgate.net/post/What_is_Co-Polarization_and_CrossPolarization_in_terms_of_both_EPlane_and_Hplane_in_HFSS/56dfec525b4952d5fa6ad713/citation/download.

[54] V. Samarthay, S. Pundir, and B. Lal, 2014. “Designing and optimization of inset fed rectangular microstrip patch antenna (RMPA) for varying inset gap and inset length”. In 2014 International Journal of Electronic and Electrical Engineering, *7*(9), pp.1007-1013.

[55] K. Ding, C. Gao, T. Yu, D. Qu and B. Zhang, 2016. “Gain-improved broadband circularly polarized antenna array with parasitic patches”. In 2016 IEEE Antennas and Wireless Propagation Letters, 16, pp.1468-1471.

[56] Prajapati, Dr. Pravin. (2016). Re: How can we ensure about the polarization type in CST simulation?. Retrieved from: https://www.researchgate.net/post/How-can-we-ensure-about-the-polarization-type-in-CST-simulation/5798afadf7b67ea4f304a451/citation/download.

[57] B. Y. U. Putri, E. S. Nugraha, A. Prakasa, S. F. Siddiq, 2020. “Design and Performance Analysis of Linear Array Microstrip Antennas with Mitered-Bends Feeding Network for X-Band Radar Applications”. In 2020 Jurnal Elektronika dan Telekomunikasi, 20(1), pp.9-15.

CST MICROWAVE STUDIO

CST STUDIO is a powerful simulation platform for all kinds of electromagnetic field problems and related applications. It provides a large package of simulation modules; one of them is CST MICROWAVE STUDIO.

CST MICROWAVE STUDIO (CST MWS) is a specialist tool for the 3D EM simulation of high frequency components. CST MWS enables the fast and accurate analysis of high frequency (HF) devices such as antennae, filters, couplers, planar and multi-layer structures and SI and EMC effects. CST software makes available Time Domain and Frequency Domain solvers, CST MWS offers further solver modules for specific applications. Filters for the import of specific CAD files and the extraction of SPICE parameters enhance design possibilities and save time. It is based on the finite integration technique (FIT). It allows to choose the time domain as well as the frequency domain approach. The Time Domain Solver calculates the broadband behavior of electromagnetic devices in one simulation run with an arbitrarily fine frequency resolution. The modeling of curved structures using the Perfect Boundary Approximation technique and the modeling of thin perfectly electric conducting sheets with the Thin Sheet Technique tries to cope with the typical difficulties inherent to classical FDTD methods [].

CST, as a general-purpose software package being a real competitor for HFSS, has gained popularity in the last few years. Also, for the analysis and design of planar and small antennas. A problem in CST is the ripples in the frequency response in case the tool box is not appropriate. This is due to the fact that the flag ship of CST is a time domain solver.

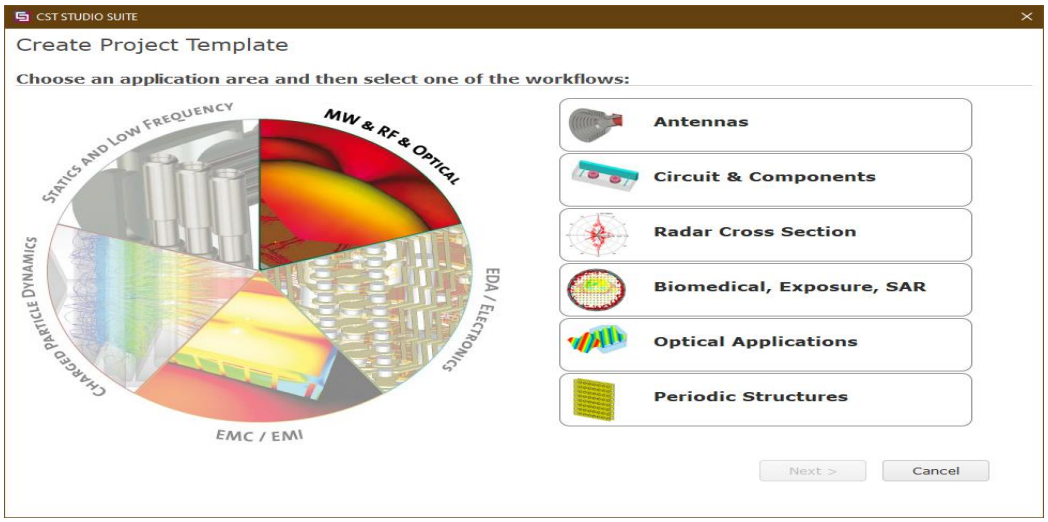

Figure A.1 CST MWS Different Applications.

APPENDIX A

CST MWS contains six different algorithms for parametric optimization. The most common, and modern one is Trust Region Framework algorithm.

Trust Region Framework is a fast and accurate optimizer that converges robustly and finds an optimum within the given parameter bounds using a low number of evaluations. It selects a local optimizing technique embedded in a trust region framework. The algorithm starts with building a linear model on primary data in a "trust" region around the starting point. Fast optimizations are done based on this local model to achieve a candidate for a new solver evaluation. The new point is accepted, if it is superior to the anchors of the model. If the model is not accurate enough the radius of the trust region will be decreased and a model on the new trust region will be created. The algorithm will be converged once the trust region radius or distance to the next predicted optimum becomes smaller than the specified domain accuracy.

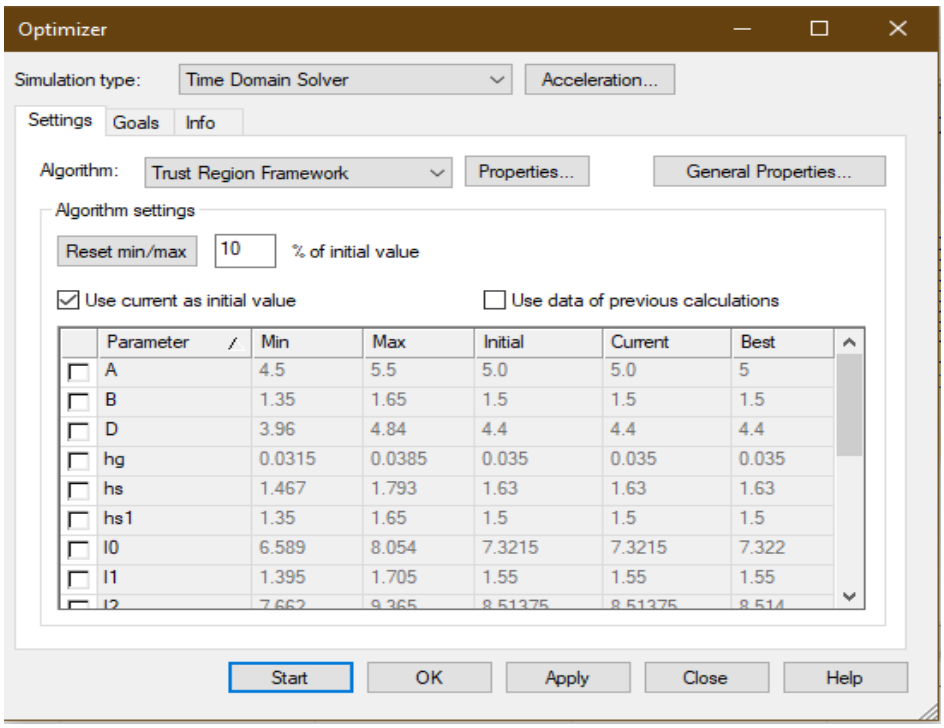

Figure A.2 CST MWS Optimizer.

APPENDIX B

Vacuum Breakdown Threshold Voltage

The DC and low RF breakdown have been addressed extensively through theory, simulations, and measurements. In contrast, gas breakdown due to high frequency time-varying fields especially in micro/nanogaps remains poorly understood and has not been described by a general scaling law. The AC breakdown problem has been studied since 1950s. A few generalizations also exist for breakdown voltage as a function of frequency-gap 'f' 'd' and pressure-gap 'p' 'd' based on vacuum experiments. These breakdown relationships, however, do not apply when the same 'p' 'd' values are obtained in GHz to THz gaps at atmospheric pressures when the excitation frequency becomes comparable with the particle collision frequency. While a few theories to calculate breakdown field in high frequencies exist in literature, these are highly restrictive when applied to micro/nanogaps [52].

Frequency domain can be classified into four distinct breakdown regimes depending on the applied frequency. A critical frequency below which the breakdown is predominantly boundary controlled thereby resembling DC breakdown was observed. At around the critical frequency, the breakdown voltage displays a sharp decrease thereby transitioning to a regime where breakdown is diffusion controlled. At very high frequencies, the electrons no longer gain sufficient energy from the field thereby unable to participate in ionizing collisions. This leads to an increase in breakdown voltage at very high frequencies depending on the gap size. The Figure A.3 shows the change of breakdown voltage with frequency [52]:

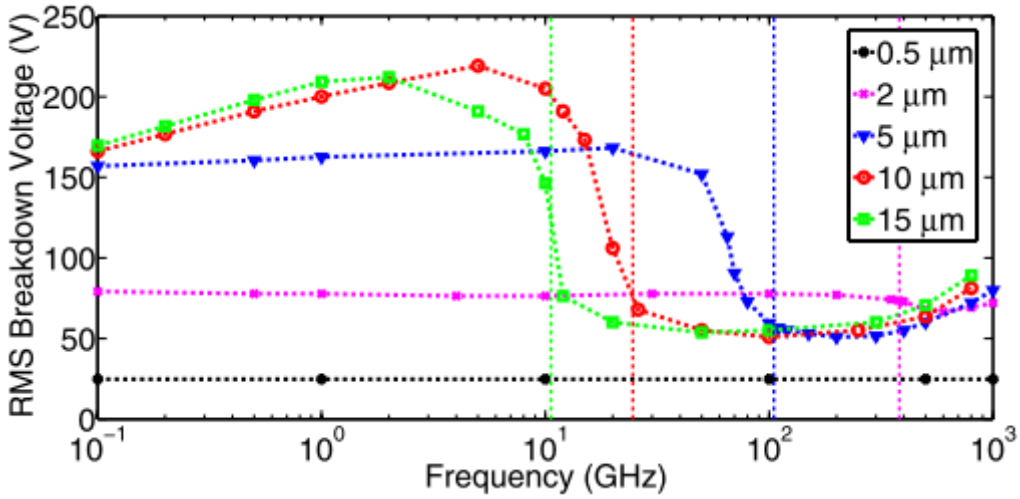

Figure A.3 Frequency Response of Breakdown Voltages and the Predicted Critical Frequency.